On the water content in CO2 + CH4 and CO2-rich mixtures: Experimental and modelling evaluation at temperatures from 233.15 to 288.15 K and pressures up to 15 MPa

Valderio de Oliveira Cavalcanti Filho, Antonin Chapoy, Rod Burgass

On the water content in CO_2 + CH_4 and CO_2-rich mixtures: experimental and modelling evaluation at temperatures from 233.15 to 288.15 K and pressures up to 15 MPa

Valderio de Oliveira Cavalcanti Filho[a], Antonin Chapoy[a,b,1] and Rod Burgass[a]

[a]*Hydrates, Flow Assurance & Phase Equilibria Research Group, Institute of Petroleum Engineering, Heriot-Watt University, UK*
[b]*MINES ParisTech, CTP-Centre Thermodynamique des Procédés, 35, Rue Saint Honoré, 77305 Fontainebleau, France*

Abstract

An experimental and modelling investigation of water content in CO_2+CH_4 and CO_2-rich mixtures in equilibrium with hydrates or liquid water was carried out at temperatures between 233.15 and 288.15 K at pressures up to 15 MPa. Some measurements were undertaken in two-phase region, in the presence of hydrates, with liquid and vapour compositions also reported. Predictions from cubic-plus association SRK, SRK incorporating NRTL with Huron-Vidal mixing rules and multiparametric EoS-CG/GERG equations of state were compared with experimental data. In comparison with pure carbon dioxide, the addition of small amounts of impurities (permanent gases and/or hydrocarbons) resulted in a significant reduction in the water content of the fluid phases present. Overall, sCPA showed good agreement with experimental data, although SRK-HV-NRTL gave better results for some cases, despite the use of only two adjustable parameters. By contrast, multiparametric EoS-CG yielded poor representation of the experimental data. In the two-phase region, no matter the equation of state used, a tendency to underestimate water content in the liquid phase was observed.

Keywords: water content, CO_2+CH_4, CO_2-rich mixtures, sCPA, SRK+HV+NRTL, EoS-CG

[1] Corresponding author. Tel.: + 44 131 451 3797
E-mail address: a.chapoy@hw.ac.uk

1. Introduction

Carbon capture and storage (CCS), enhanced oil recovery (EOR) using alternate gas and water (WAG) injection, sour-gas-associated oil reservoirs exploration, dense phase transportation and subsea processing are only a few cases where, nowadays, CO_2-rich systems play an important role. In most of these situations, fluid phases encounter low temperatures and high pressures, as new technologies made possible the exploration of remote areas, namely in ultradeep water, such as the Brazilian pre-salt. The development of the production in such new frontiers demands carbon dioxide separation, conditioning, compression and final disposal.

Specifications for water content for such systems depend on several aspects. According to John Carrol [1], in the United States, the value is usually 7 lb/MMCF (about 112 kg/MM std m^3), whereas in Canada, it is 4 lb/MMCF (about 65 kg/MM std m^3), which might represent dew points as low as 235 K, at atmospheric conditions, depending on the gas composition. In Europe, EASEE-gas has a limit of 265.15K for dew points, referenced to a pressure of 7 MPa. Due to the requirement for transportation through subsea pipelines, offshore drying units might have higher specifications in order to prevent water condensation and hydrate formation.

In Brazilian offshore scenario, for instance, Andrade et al. [2] mentioned a specification of 2 lb/MMCF (circa 32 kg / MM std m^3) for the exported treated gas from standard FPSO units operating in the deep water Campos Basin. For the recently discovered pre-salt fields, however, the authors presented a more detailed description of surface facilities designed to handle inlet natural gas streams containing up to 30% of CO_2 which are dehydrated to a specified water content as low as 1 ppmv, using molecule sieves. In addition, the description also includes membrane systems that are used to remove carbon dioxide from natural gas streams (maximum 5% CO_2), en route to further processing in onshore liquid recovery plants, and produces a secondary stream with high CO_2 concentration (up to 90% mole/mole) destinated to reservoir reinjection. These units, and other process facilities dealing with CO_2-rich mixtures, may experience low temperatures during pressure drop (e.g., through valves, restrictions or porous media flow during WAG

injection), blowdown (controlled emptying) or depressurisation (accidental rupture) events. In all these occurrences, phase transitions can take place and the presence of water might lead to hydrate formation, resulting in partial or total blockages.

Accurate water content predictions are of utmost importance for the above-mentioned processes. Predictions are required in order to dictate design and operation of dehydration units and/or inhibitor injection pumps. Despite recent advances, no reliable model for both high pressure and low temperature involving associative molecules (such as water and carbon dioxide) is available. In addition, there is a lack of experimental data which contributes to a tendency to overlook the influence of minor impurities.

Measurements for water content in CO_2 rich-mixtures are mainly restricted to CH_4 – CO_2. Table 1 details the majority of data published to date [3–18]. Composition for all fluid phases present are rarely reported and, instead, material balance, correlation predictions or dry basis data are commonly presented. The work of Al Ghafri et al [15] is the only exception, where vapour-liquid-liquid (VLLE), vapour-liquid (VLE) and liquid-liquid (LLE) equilibrium compositions have been reported. Data for the upper quadruple point (H-L_w-L_{CO2}-V) for a wide range of carbon dioxide concentration are also available [5,15,17,19].

CH_4-H_2O and CO_2- H_2O mutual solubilities have been investigated over a wide range of temperature and pressures [20–65]. Essential for parameter fitting purposes, these data have been correlated using different equations of state (EoS). Huron Vidal mixing rules [66] with Soave-Redlich-Kwong (SRK) and NRTL Gibbs excess energy (G^{ex}) model (SRK-HV-NRTL) was used by Pedersen et al. [67] and Austegard et al. [68] . While Pedersen et al. applied this model to water – reservoir hydrocarbons equilibrium at high temperature (308.15 – 473.15 K) and pressures (70 – 100 MPa), Austegard et al. compared the SRK-HV-NRTL model with the simplified Cubic plus Association model proposed by Kontogeorgis et al. [69,70]. The latter used predictions for mutual solubilities between water, CO_2 and CH_4 and concluded that the SRK-HV-NRTL model can produce acceptable results, while sCPA has been found less accurate. Also, the Peng-Robinson coupled with the Wong-Sandler approach with NRTL (PR-WS-NRTL) was tested by Valtz et al. [71] and Yang et al. [72]. High deviations between CO_2 solubility and PR-WS-NRTL results were observed by Valtz and co-workers, particularly at pressures above 8 MPa. Yang et al. (2019) have found compatible predictions from sCPA and SRK-HV-NRTL models for gas condensate mixtures with water. Gernert and Span [73]

extended the original GERG-2008 model for humid and CO_2-rich gases. Later, a new version extended to combustion gases (EOS-CG) was reported as accurate for VLE predictions for mixtures including water, CO_2 and CH_4, covering a wide temperature and pressure range [74].

Recently, a broader comparative study for CO_2 – water was performed by Aasen et al. [75]. The authors have fitted and tested predictions from traditional Peng-Robinson (PR) and Soave-Redlich-Kwong (SRK), using Twu et al. [76] alpha function, EoS/G^{ex} models (PR and SRK with HV[77]/WS[78] using classic or TWU-α functions), equations that include association terms (sCPA [69,70] , sCPA-PR [79] and PC-SAFT [80], all of them using different association schemes for water), multiparametric EoS (GERG-2008 [81] and EoS-CG [73,74]) and predictive models (PR-UMR [82] and VTPR [83]). An extensive data selection and evaluation was carried out and only accepted measurements between 273 – 478 K and at pressures below 61 MPa were used. According to their findings, at least three fitting parameters are required to represent the binary mixture within an accuracy of 10%. Moreover, the PR/HV with the Twu alpha function and volume shift correction was reported as being the most accurate model considering phase compositions and densities [75]. More recently, Yang et al. [84] used PR and the Wong-Sandler (WS) mixing rules with NRTL to deal with CO_2/water and oil in compositional flooding simulations. Despite the good results, a very limited range of pressures and temperatures were studied.

Table 1. Data published for $CH_4 – CO_2 –$ water.

Temperature (K)		Pressure (MPa)		CO_2 % mole range (dry basis)		Equilibrium Conditions	Type of Data			Reference
min	max	min	max	min	max		Water content	Solubility Data	Gas in Hydrate Phase	
293.15	313.15	3	6	10	50	VL_wE	yes	no	no	[3]
344.15		10	100	17.4	94.13	VL_wE	no	yes	No	[4]
324	376.2	10.5	50.6	34	62	VL_wE	yes [(a)]	yes	No	[11]
288.71	323.15	5.559	7.517	94.69		VL_wE Three Phase Locus	yes	no	no	[12]
243.1	288.4	0.11	6.05	20	70	VL_wE	yes[(b)]	no	no	[13]
304.26	473.15	3.45	103.42	10	70	VL_wE $VL_wL_{CO2}E$	yes	no	no	[14]
285.15	300.5	4.963	20	49	99	VL_wE Four Phase Locus $L_wL_{CO2}E$	yes	yes	no	[15]
273.6	284.2	1.51	7.19	22.5	76.1	HL_wV	no	yes	yes	[16]
283.32	285.76	4.412	7.251	79.74	100	Four Phase Locus	no	no	yes	[19]
280.3		3.04	5.46	0	100	HL_wV	no	yes	no	[10]
274.02	280.05	1.66	4.03	28.3	61.2	HL_wV	no	yes	no	[18]
273.16	283.26	1.5	5	0	100	HV HL_wV Four Phase Locus	no	no	yes	[17]
283.09	287.04	4.46	8.37	78	100	Four Phase Locus	no	no	no	[5]
323.15		10		19	93	VL_wE	no	yes	no	[8]
310.23	344.67	6.99	13.89	11.32	20.22	VL_wE	yes	no	no	[7]
285.11	288.39	7.17	27.71	84.6	90	HL_wL_{CO2}	no	yes	no	[9]

(a) Data calculated by model.

(b) Reported as dew point temperatures

No similar comparative study has been published for water content predictions for CH_4+CO_2 systems. Predictions from PR-CPA [85], sCPA [85,86], PR and SRK with asymmetric mixing rules [87], PC-SAFT [88,89], SAFT-VR [15,86], SAFT-γ Mie group contribution[90], Peng-Robinson-Stryjek-Vera (PRSV) with WS mixing rules and NRTL[91,92] have been individually analysed. Al Ghafri et al. [15] has found that the SAFT-VR model presented by Míguez et al. [93] strongly underestimated solubilities in aqueous phase while water content in vapour phase is overpredicted. Some models were only evaluated for temperatures above 273.15 K, for instance, the PRSV-WS-NRTL with a linear composition dependent function presented by Zhao and Lvov [91,92].

Moreover, in the case of water content in CO_2-rich multicomponent mixtures, the capabilities of different models to predict phase changes based on parameters fitted from binary data are rarely mentioned and hardly discussed. Perhaps partially because of the absence of published data, partially due to a natural tendency to oversimplify such mixtures as pure carbon dioxide or, at best, carbon dioxide – methane. In a previous study, Chapoy et al. [94] have highlighted some problems with such approaches.

In the present paper, an experimental and modelling investigation into CH_4 - CO_2 and multicomponent CO_2-rich mixtures in equilibrium with hydrates or liquid water is described. Equations of state representing the most promising approaches to calculate water content in natural gas components were evaluated. It includes association theory (sCPA), G^{ex}/EoS mixing rules (SRK-HV-NRTL) and highly accurate multiparametric (EoS-CG GERG version) thermodynamic models. A parametrization procedure that included data in hydrate region was used to obtain new fitted parameters for SRK-HV-NRTL. Model predictions were compared with experimental water content data measured for CO_2 + CH_4 (25/75, 50/50 and 75/25 initial ratio) and multicomponent mixtures (containing at least 38.65% of CO_2, light hydrocarbons, up to i-C_5, and permanent gases, which included nitrogen, oxygen, argon and hydrogen) carried out at temperatures between 233.15 and 288.15 K and pressures up to 15 MPa. Measurements in the two phase-region in the presence of hydrates were also conducted and complete compositions are presented for the liquid and vapour phases. Water content predictions in both phases were also compared with model predictions.

2. Experimental Methods

2.1. Materials

Carbon dioxide and methane used in these experiments were 99.99% pure, supplied by BOC (Table 2). Methane/Carbon Dioxide mixtures (1:3, 1:1 and 3:1) were gravimetrically prepared from pure components.

Table 2. Composition of the chemical used in this work

Chemical	Symbol	CASRN	Purity	Supplier
Carbon dioxide	CO_2	124-38-9	99.99 vol%	BOC
Methane	CH4	74-82-8	99.99 vol%	BOC

All the CO_2-rich synthetic mixtures (referred to as MIX 1, 2, 3 and 4) were prepared by BOC and their compositions are given in Table 3. De-ionized water was used in all tests.

Table 3. Composition, mole% each component, of the multicomponent mixtures used in this work. Uncertainties are given in brackets.

Component	MIX 1	MIX 2	MIX 3	MIX 4
CO_2	Balance (95.36)	Balance (38.65)	Balance (96.07)	Balance (69.3)
Methane	-	41.30 (±2.06)	-	26.2 (±0.5)
Ethane	-	-	-	0.93(±0.02)
Propane	-	-	-	0.290(±0.006)
n-Butane	-	-	-	0.070(±0.001)
i-Butane	-	-	-	0.070(±0.001)
n-Pentane	-	-	-	0.020(±0.0004)
i-Pentane	-	-	-	0.0300(±0.0006)
Nitrogen	3.0 (±0.1)	20.05 (±1.06)	1.92 (±0.04)	3.08 (±0.06)
Hydrogen	-	-	0.60 (±0.01)	-
Oxygen	10.6 ppm (±0.5)	-	0.83 (±0.02)	-
Argon	1.59 (±0.03)	-	0.58 (±0.01)	-

2.2. Water content measurement set-up

The equipment is comprised of an equilibrium cell and a set-up for measuring the water content of equilibrated fluids flowing out of the cell. A schematic of the set-up is shown in Figure 1. The equilibrium cell is a 300 ml, Titanium piston vessel rated to 69 MPa. The cell is surrounded by a jacket which is connected to a temperature-controlled circulator. The circulator can control the temperature of the fluid pumped through the jacket within ±0.1 K of the set-point and can be used at temperatures between 183.15 and 373.15 K. The

cell temperature is measured using a PRT (Platinum Resistance Thermometer) located in the jacket. The cell pressure is measured using a strain gauge pressure transducer mounted on the lower end of the cell. The difference between the temperature probe in the jacket and the temperature inside the cell was checked against a platinum resistance probe that has a certificate of calibration issued in accordance with NAMAS Accreditation Standard and NAMAS Regulations. The pressure transducer is regularly checked for accuracy using a Budenberg dead weight tester.

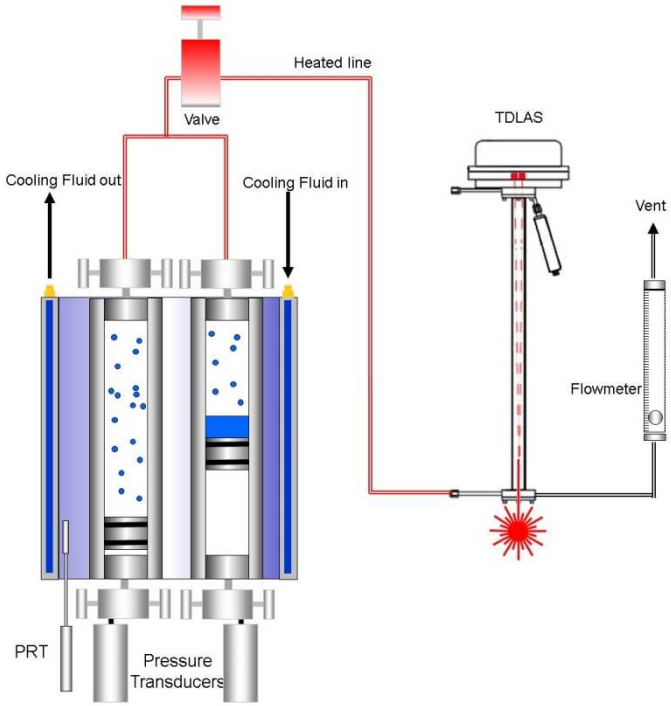

Figure 1. Schematic diagram showing equilibrium cell and water content measurement set-up arrangements.

The moisture content set-up is comprised of a heated line, a tuneable diode laser absorption spectrometer (TDLAS) and a flow meter. A TDLAS for accurate water content measurements from Yokogawa (Figure 1) was used in this work. The unit is constructed of polished Monel and thus can be used with corrosive gases such as H_2S. The set-up is such that a tuned infrared source is passed through the test sample to a detector. The measurement of water content is based upon true peak area and therefore, unlike other units which use peak height, it is not influenced by changes in background gas. This is subject to the manufacturer specifications regarding the range of concentrations of different gases that will not interfere with the accuracy of the measurements. The unit has

two measurement ranges 0-100 ppmV and 0-3000 ppmV, both having a stated accuracy of ±1% of full scale.

2.3. Procedures

At the start of a test around 10 ml of 0.1 mm glass beads are placed in a cup shaped depression in the bottom of the piston. 2 ml of deionised water are then mixed with the glass beads. The glass beads have been found to aid in formation and dissociation of hydrates in previous work, helping to achieve equilibrium [95]. The cell is then closed, and the temperature reduced to 263.15 K and evacuated before injecting the fluid. The cell temperature and pressure are then adjusted to achieve the desired test conditions. The cell temperature is then cycled to lower and higher temperatures than the set point over at least 20 hours. This has been confirmed as being sufficient time for equilibrium to be achieved by conducting water content measurements over a number of days in one test.

Once equilibrium had been achieved the valve at the top of the cell was opened in order to fill the section of heated line up to the valve prior to the hygrometer at the same time nitrogen was introduced into the base of the cell in order to maintain the pressure constant. Following this, the valve prior (inlet) to the TDLAS was opened sufficiently to achieve a flow rate of between 0.5 and 1 litre per minute through the spectrometer. The water content reading from the hygrometer was then monitored until it was stable for at least 10 minutes. This was then taken as the moisture content of the equilibrated fluid in the cell (i.e., flowing out of the cell). During sampling the heated line was maintained at a temperature of 463.15K. The overall estimated experimental accuracy is 4% of the reading, for water content above 100ppmV, and ± 2 ppmV for values below.

2.4. Two-phase region analysis

In tests where both liquid (L) and vapour (V) phases were present in equilibrium, a sample of the fluids coming from the test cell was collected in an evacuated cylinder and subsequently analysed using GC. Details of the calibration procedure for the GC are shown below.

The Flame Ionisation Detector (FID) was used to detect the hydrocarbons (methane, ethane, propane, i-butane, n-butane, pentanes). For calibration, pure gases are simply

injected in the chromatograph via the injector with gas syringes of given volumes: 500-µl syringe for methane calibration and a 100-µl syringe for ethane. For heavier hydrocarbons (propane to pentanes), MIX 4 was used for calibration. Calibration curves for the different hydrocarbons are obtained, that is a relationship between the response of the detector and the injected quantity.

Comparison between injected quantities and calculated quantities (after adjustment of the parameters of polynomial expressions) allows estimation of the calibration uncertainty, which is in a range of ± 0.8% for methane (second order polynomial adjustment), of ±1.2% for ethane (first order polynomial adjustment) and of ± 2 % for propane to pentanes (first order polynomial adjustment). NB: iso-pentane and n-pentane were calibrated and analysed together as a single component.

The Thermal Conductivity Detector (TCD) was used to detect N_2 and CO_2. For calibration, the same procedure was used, the gases are simply injected in the chromatograph via the injector with gas syringes of given volumes: 500-µl syringe for CO_2 calibration and a 100-µl syringe for Nitrogen. Comparison between injected quantities and calculated quantities allows estimation of the calibration uncertainty, which is in a range of ± 1 % for CO_2 (second order polynomial adjustment), of ± 0.8% for Nitrogen (first order polynomial adjustment).

3. Thermodynamic Modelling

A representative range of equation of states relevant to industrial applications were used in this study. The choice included one association theory model (sCPA), one EoS with G^{Ex} mixing rules and one highly accurate multiparametric GERG, extended to combustion gases (EoS-CG).

3.1. Simplified Cubic-plus Association SRK (sCPA)

A widely used simplified version of Soave-Redlich-Kwong Cubic Plus Association (sCPA), originally presented by Kontogerogis et al.[69,70] was used for this study. The pressure-explicit expression for the model is given by:

$$P = \frac{RT}{v-b} - \frac{a}{v(v+b)} - \frac{1}{2}\frac{RT}{v}\left(1 + \rho\frac{\partial \ln g}{\partial \rho}\right)\sum_{i=1}^{N} x_i \sum_{A_i}(1 - X_{Ai}) \quad (1)$$

where x_i is mole fraction of the component i and X_{Ai} represents the mole fraction of molecule i not bonded to the site A and expressed as:

$$X_{A_i} = \left(1 + \sum_j \sum_{B_j} x_j X^{B_j} \Delta^{A_i B_j}\right)^{-1} \quad (2)$$

where $\Delta^{A_i B_j}$ represents the association strength between site A on molecule i and site B on molecule j and is defined as:

$$\Delta^{A_i B_j} = g \quad (d)\left[exp\left(\frac{\varepsilon^{AB}}{RT}\right) - 1\right] b\beta^{A_i B_j} \quad (3)$$

where ε and β are the association energy and volume, respectively. Parameter values for water have been previously published[95]. The simplified expression of the radial distribution, g(d), adopted by Kontogeorgis et al[70] was used:

$$g \quad = \frac{1}{1 - 0.475\frac{b}{v}} \quad (4)$$

In the present work, a four site (4C) association scheme was adopted for water. It considers that hydrogen bonding can occur between the two hydrogen atoms and the two lone pair of electrons in the oxygen atom. A cross-associative approach was adopted to the carbon dioxide molecule.

The energy parameter (*a*) of the SRK-CPA is defined using a classical Soave-type temperature expression:

$$a = a_0\left[1 + c_1\left(1 + \sqrt{T_r}\right)\right] \quad (5)$$

where parameters a_0 and c_1, in the case of associative molecules, were adjusted for single component using vapour pressure data obtained from open literature and previously published[95]. Co-volume is assumed as temperature independent and is also adjusted for single component using saturated liquid volume data for associative molecules. For the non-

associative ones, traditional SRK expression for a_i and b_i based on critical point coordinates were used.

The extension to mixtures is made using the classical van der Waals mixing rules expressions modified to include binary interaction parameters (BIPs). These were correlated to experimental data. Cross association parameters are obtained from CR-1 combining rules.

3.2. Soave-Redlich-Kwong / Huron-Vidal / NRTL model (SRK/HV/NRTL)

The Huron-Vidal mixing rules were applied to incorporate the NRTL Gibbs excess energy to the Soave-Redlich-Kwong equation[66] . The starting point is given by:

$$a = b\left[\sum_{i=1}^{C} x_i \frac{a_i}{b_i} - \frac{G^{ex}{}_{model}}{q_{eos}}\right] \tag{6}$$

where q_{eos} = ln 2 for SRK. The traditional expression is employed to **b**:

$$b = \sum\sum x_i x_j \frac{b_{ii} + b_{jj}}{2} \tag{7}$$

For an improved pure component vapour pressure prediction, Mathias-Copeman-like alpha functions[96] were fitted for water and carbon dioxide, according to Equation 8:

$$\alpha = \left[1 + c_1\left(1 - \sqrt{T_r}\right) + c_2\left(1 - \sqrt{T_r}\right)^2 + c_3\left(1 - \sqrt{T_r}\right)^3\right] \tag{8}$$

Values for c_1, c_2 and c_3 are reproduced in Table 4.

Table 4. Parameters for Mathias-Copeman alpha function, Equation 8, used in this work.

	Carbon Dioxide		Water
	$T_r \leq 1$	$T_r > 1$	
C_1	0.880929	0.880929	1.09442
C_2	-0.879632	0	-0.67481
C_3	3.326455	0	0.691994

Originally, Huron and Viral[66] used a version of NRTL using local composition as corrected volume fractions, which leads to the introduction of the co-volume in the calculation of c_{ij}:

$$\frac{G^{ex}}{RT} = \sum_{i=1}^{c} \frac{\sum_{j=1}^{c} x_j \tau_{ji} c_{ji}}{\sum_{k=1}^{c} x_k c_{ji}} \quad (9)$$

where,

$$c_{ji} = b_j e^{(-\alpha_{ji}\tau_{ji})} \quad (10)$$

and $\alpha_{ii} = \tau_{ii} = 0$.

One of the main advantages of such choice for the g^E model is that an exact reduction to the classical mixing and combining rules can easily be obtained by setting:

$$\alpha_{ji} = 0 \quad (11)$$

$$\tau_{ji} = \frac{q_{eos}}{RT}\left[-2\frac{\sqrt{b_i b_j}}{b_i + b_j}\sqrt{\frac{a_i}{b_i}\frac{a_j}{b_j}}\left(1 - k_{ij}\right)\right] \quad (12)$$

Apart from CO_2/water, CH_4/water and CO_2/CH_4, to which τ_{ij} and τ_{ji} were fitted using data available on the literature, Equations 11 and 12 were applied to recover traditional the SRK model. For this case, binary interaction parameters were taken from Jaubert and co-workers Group Contribution approach [97] which was extended to SRK in [98].

3.3. GERG-2008 /EOS-CG

The original GERG-2008 wide-range equation of state for natural gases was published by Kunz and Wagner[81] for 21 components including methane and carbon dioxide. The general structure of this multiparametric model is explicitly expressed in term of dimensionless Helmholtz energy ($\alpha = a/RT$) split into ideal (α^o) and residual (α^r) contribution terms:

$$\alpha(\delta, \tau, x) = \alpha^o(\rho, T, x) + \alpha^r(\delta, \tau, x) \quad (13)$$

for which, reduced mixture density (δ) and inverse reduced mixture temperature (τ) are defined as:

$$\delta = \frac{\rho}{\rho_r} \tag{14}$$

$$\tau = \frac{T_r}{T} \tag{15}$$

Reduced properties ρ_r and T_r are composition dependent and given by, respectively:

$$\frac{1}{\rho_r(x)} = \sum_{i=1}^{C} x_i^2 \frac{1}{\rho_{c,i}} + \sum_{i=1}^{C-1} \sum_{j=i+1}^{C} 2x_i x_j \beta_{v,ij} \gamma_{v,ij} \frac{x_i + x_j}{\beta_{v,ij}^2 x_i + x_j} \frac{1}{8} \left(\frac{1}{\rho_{c,i}^{1/3}} + \frac{1}{\rho_{c,j}^{1/3}} \right)^3 \tag{16}$$

$$T_r(x) = \sum_{i=1}^{C} x_i^2 T_{c,i} + \sum_{i=1}^{C-1} \sum_{j=i+1}^{C} 2x_i x_j \beta_{T,ij} \gamma_{T,ij} \frac{x_i + x_j}{\beta_{T,ij}^2 x_i + x_j} \left(T_{c,i} T_{c,j} \right)^{1/2} \tag{17}$$

where $\beta_{v,ij}$, $\gamma_{v,ij}$, $\beta_{T,ij}$ and $\gamma_{T,ij}$ are binary parameters adjusted to experimental data and obey the following relations:

$$\beta_{v,ji} = \frac{1}{\beta_{v,ij}} \tag{18}$$

$$\beta_{T,ji} = \frac{1}{\beta_{T,ij}} \tag{19}$$

$$\gamma_{v,ji} = \gamma_{v,ij} \tag{20}$$

$$\gamma_{T,ji} = \gamma_{T,ij} \tag{21}$$

The ideal representation of Helmholtz energy is given in terms of ideal gas mixture:

$$\alpha^o(\rho, T, x) = \sum_{i}^{N} x_i [\alpha_{oi}^0(\rho, T) + ln x_i] \tag{22}$$

A dimensionless form of the Helmholtz ideal-gas state, $\alpha_{oi}^{0}(\rho,T)$, is presented by Kunz and Wagner[81]. Additionally, the residual part is split into a general ideal gas residual contribution, $\alpha_{oi}^{r}(\delta,\tau)$, and a binary specific residual function, $\alpha_{ij}^{r}(\rho,\tau)$, as follows:

$$\alpha^{r}(\rho,T,x)=\sum_{i}^{N}x_i\alpha_{oi}^{r}(\delta,\tau)+\sum_{i}^{N+1}\sum_{j=i+1}^{N}x_ix_jF_{ij}\alpha_{ij}^{r}(\rho,\tau) \quad (23)$$

Binary specific residual functions are normally expressed as a polynomial expression that also includes exponential terms. Different formats have been introduced, and a generalized form is presented by Herrig [74]. Any specific function was originally included in the GERG-2008 formulation for water binary mixtures. Later, Gernert and Span [99] introduced an extended form for humid gases and carbon capture and storage (CCS) mixtures. This extension, named EoS/CG, included specific residual functions for CO_2/ water (validated for 251-623 K and 1 – 350 MPa range for VLE data). Recently, Herrig [74] developed a binary specific departure function for methane/water. For model tuning, the author used data for methane solubility, water content and validation were performed in the temperature range of 250 and 600 K and pressure up to 68.8 MPa. Thus, for the aim of this work, values for $\beta_{v,ij}, \gamma_{v,ij}$, $\beta_{T,ij}$ and $\gamma_{T,ij}$ as well as binary specific functions expressions were taken from the works of Kunz and Wagner [81], Gernert and Span [99] and Herrig [74].

Hydrate phase and hydrate forming conditions are modelled by the solid solution theory of van der Waals and Platteeuw, as implemented by Parrish and Prausnitz. A detailed description of the thermodynamic methodology as well as parameter values was previously presented [95].

4. Results

4.1. Adjustment for SRK/HV Model

A new fitting was carried out for SRK-HV-NRTL model, for the temperature interval between 243.15 and 423.15 K and pressures up to 100 MPa. For this purpose, data for the binary systems CO_2/CH_4, CO_2/H_2O and CH_4/H_2O from several authors, including LL and VL including hydrates region, were collected, deemed and selected to avoid off-trend and inconsistent measurements[20–65]. The lack of reliable data limited the lower temperature

to 243.15 K, although, in the following sections, comparisons at 233.15 K are performed. However, such extrapolations are regarded as an important step for model evaluation, to investigate its ability to provide reasonable predictions outside fitting temperature and pressure ranges.

For methane and carbon dioxide, the following temperature independent parameter values were obtained: $\alpha = 0.4779$, $\frac{\tau_{ij}}{RT} = 0.8868$ and $\frac{\tau_{ji}}{RT} = 0.6136$. For the other pairs involving water, temperature dependent τ_{ij}were fitted and 3rd order polynomial expressions are reported in Table 5. Parameters for any component not mentioned in Table 5 was described using Equations 11 and 12 to reduce the model to the original SRK cubic equation.

Table 5. Adjusted parameters for SRK-HV-NRTL for water pair with methane or CO_2.

	Water(j)
Methane(i)	$\alpha = 0.05$ $\frac{\tau_{ij}}{RT} = -8.171 \cdot 10^{-7}T^3 + 9.994 \cdot 10^{-4}T^2 - 0.4485\mathrm{T} + 81.36$ $\frac{\tau_{ji}}{RT} = 4.861 \cdot 10^{-7}T^3 - 5.656 \cdot 10^{-4}T^2 + 0.2347\mathrm{T} - 37.68$
Carbon Dioxide(i)	$\alpha = 0.03$ $\frac{\tau_{ij}}{RT} = -1.559 \cdot 10^{-6}T^3 + 1.829 \cdot 10^{-3}T^2 - 0.7493\mathrm{T} + 118.657$ $\frac{\tau_{ji}}{RT} = 8.444 \cdot 10^{-7}T^3 - 9.624 \cdot 10^{-4}T^2 + 0.3858\mathrm{T} + 62.534$

The adjusted model was then compared with experimental data, as depicted in Figure 2 a – h. In general, a good agreement between the SRK-HV-NRTL predictions and experimental data was found for the CH_4/CO_2 binary system (Figure 2a), water content in liquid and vapour CO_2 (Figure 2b – 2c), CO_2 solubility in water (Figure 2d), water content in vapour CH_4 (Figure 2f) and CH_4 solubility in water (2g). Figures 2b and 2e show satisfactory results for fluid phase equilibrium with hydrates. Note that some limitations in dealing with liquid-liquid CO_2-water equilibrium in the vicinity of carbon dioxide critical point (T_c = 304.13K) were also observed.

Despite the results obtained for binary systems, when the model was extrapolated to predict water content for CO_2 – CH_4 mixtures, the results were unsatisfactory, see Figure 2h. It was particularly unexpected since neither high carbon dioxide concentration (z_{CO2} = 10 – 50% mole/mole) nor extreme conditions (3 – 6 MPa and 293.15 and 313.15 K) are used (data from Chapoy et al. [3]).

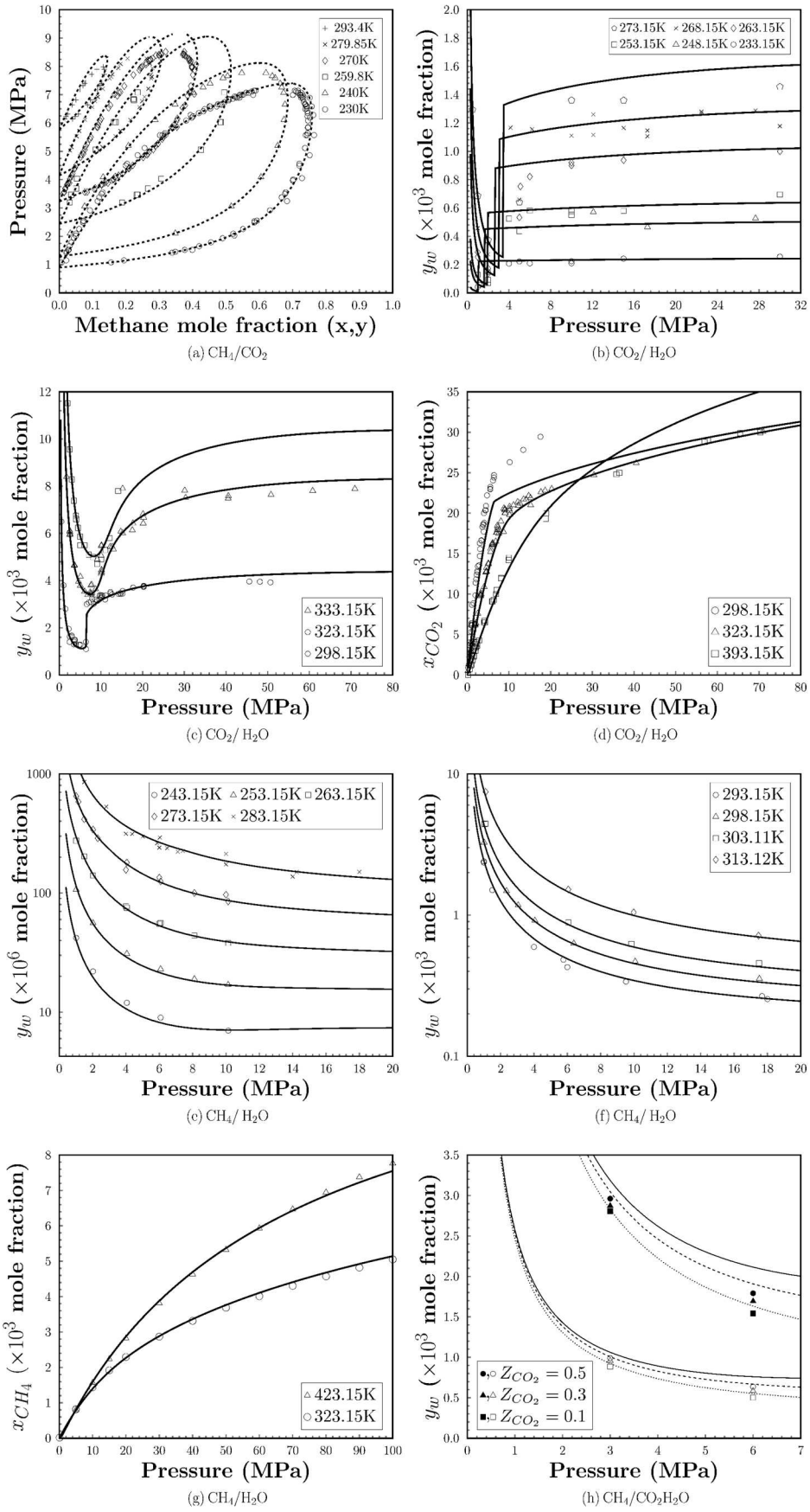

Figure 2. Predictions from adjusted SRK/HV/NRTL model. Data from:(a) [26,43,54,61–65] **(b)** [21,22,32]**., (c)** [27–31,33–35,55] **(d)** [15,27,31,33,36–38,40,41,48–53,59,71]**;(e)** [23,24,56]**, (f)** [23,24,56–58] **(g) Duan and Mao** [60,100] **(h) Chapoy et al.** [3]**.**

Further evaluations were carried out using a different set of data published by Burgass et al. [101] for a 9% CO_2/CH_4 mixture, at low temperatures, in equilibrium with hydrates. As plotted in Figure 3, the model was unable to reproduce water content measurements using the fitted parameters obtained for the binary corresponding mixtures. In fact, it showed a clear trend to overestimate values.

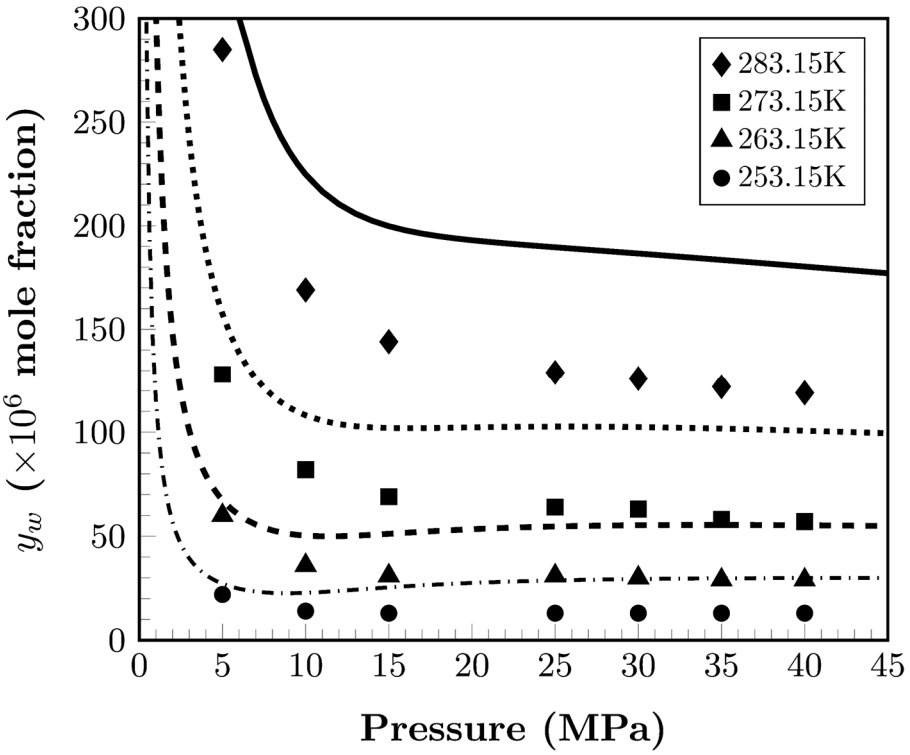

Figure 3. Water content predictions for 9% CO_2/Methane mixture at several temperatures. Data from Burgass et al. [101]**. For this set of data, AAD = 65%.**

One might attribute these limitations to self or cross-associations and the inability of SRK-HV-NRTL to properly describe them. To clarify this, predictions and experimental data for a 9%C_2H_6/CH_4 mixture (for which there is no cross-association), at the same conditions, were compared. Prior to this, a fitting for the ethane – water system was conducted, and the polynomial expression is shown in Table 6.

Table 6. Adjusted parameters for Ethane/Water using data from Chapoy et al. [99].

	Water(j)
Ethane (i)	$\alpha = 0.05$ $\frac{\tau_{ij}}{RT} = 1.807 \cdot 10^{-4}T^2 - 0.18\mathrm{T} + 53.237$ $\frac{\tau_{ji}}{RT} = -5.717 \cdot 10^{-5}T^2 + 0.06244\mathrm{T} - 21.564$

Water content in ethane was well represented using the parameters from Table 6 (Figure 4a). When extrapolated to the ternary mixture, although over predictions were observed at higher pressures, (Figure 4b), average deviations were considerably lower (ADD = 15% against 65% for 9%CO_2/CH_4). It could indicate that Huron-Vidal mixing rules fail to account for water – carbon dioxide cross-association.

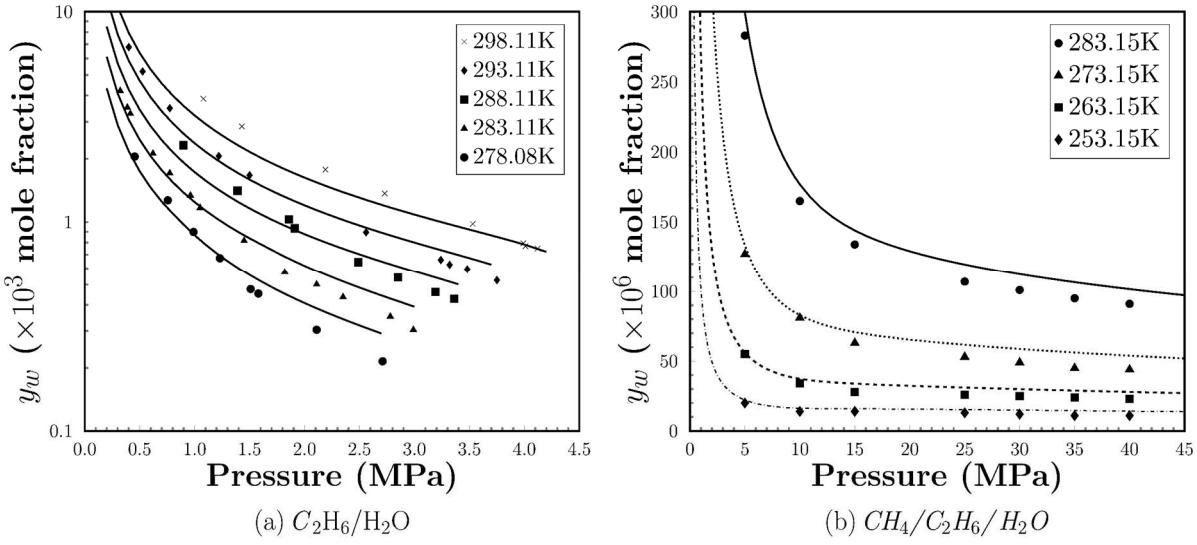

(a) C_2H_6/H_2O (b) $CH_4/C_2H_6/H_2O$

Figure 4. Predictions from SRK/HV/NRTL, data from (a) Chapoy et al. [99]. and (b) Burgass et al. [101]**.**

At this point, the fact that no adjustment was performed to methane-ethane (instead, original SRK was used) and yet good predictions were obtained suggested that the same should be used for methane-carbon dioxide. Thus, as an alternative approach, Equations 11 and 12 were adopted to recover original SRK model for CH_4/CO_2 pair, instead of employing the fitted α, τ_{ij} and τ_{ji}. Contrary to expectations, this shift gave better predictions, as seen in Figure 5. As can be seen the average absolute deviation (AAD) reduced very significantly from 65% to 23%. This is a considerable improvement and indicates that using Huron-Vidal

approach only to binary involving water is enough to guarantee the best SRK-HV-NRTL performance. Therefore, this approach was adopted for the remaining sections of this work.

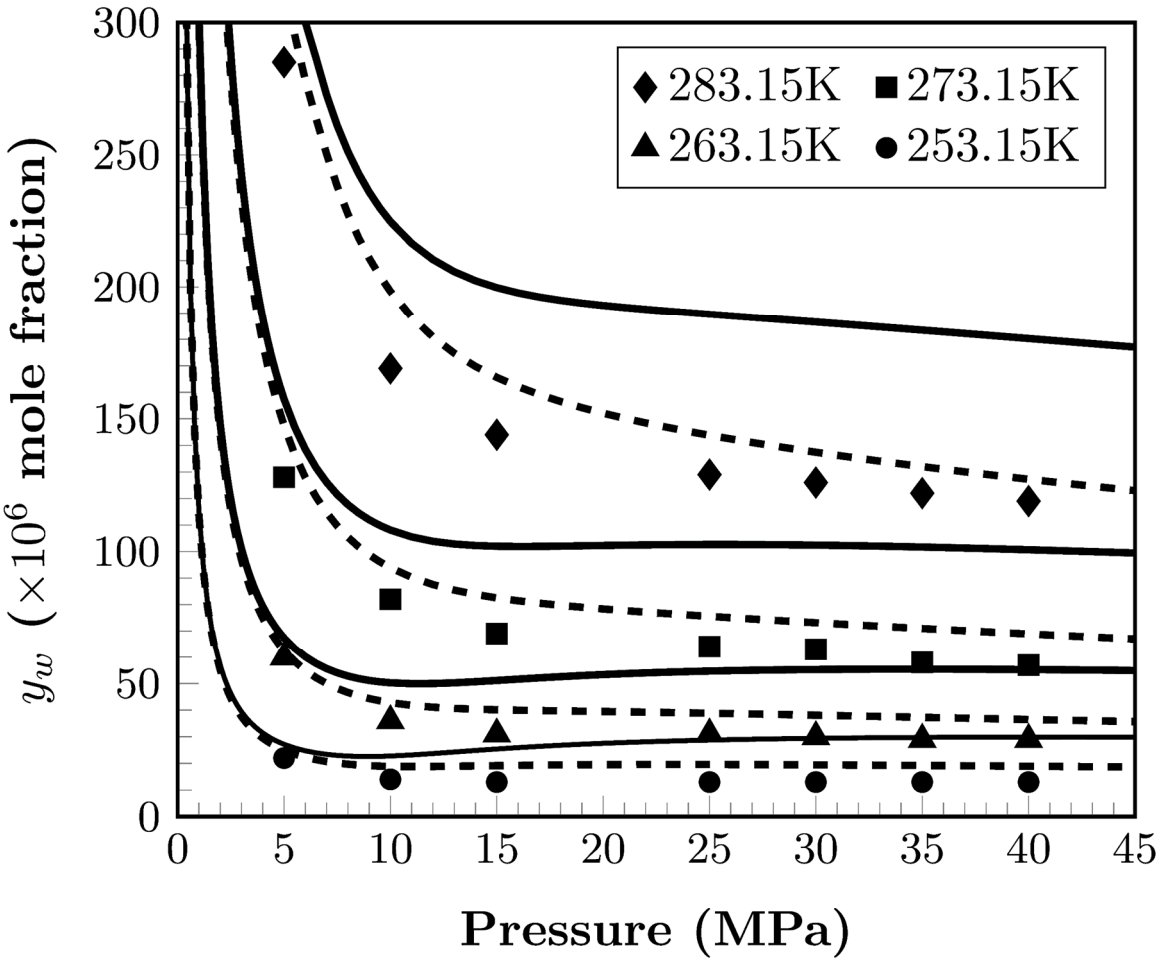

Figure 5. Comparison between predictions from two different SRK-HV-NRTL approaches: (a) Solid lines represent those obtained using $\alpha = 0.4779$, $\frac{\tau_{ij}}{RT} = 0.8868$ and $\frac{\tau_{ji}}{RT} = 0.6136$ for carbon dioxide – methane; (b) Dashed lines represent those obtained using Equations (11) and (12) approach to carbon dioxide – methane. Data from Burgass et al. [101]**.**

4.2. Water content measurements for methane/carbon dioxide mixtures

New measurements for water content in methane/carbon dioxide mixtures were carried out at temperatures between 233.15 and 288.15 K at 15 MPa. In this work, evaluations were focused in the supercritical and liquid region for which no data are available. Results are presented in Table 7.

All measurements for the 75 mole% CH_4 systems were carried above the critical point in the supercritical region. As expected, the water content is increasing with the CO_2

concentration in the feed gas, reducing with CH_4 content, i.e., 92%, 81 % and 55% average reduction compared to pure CO_2 in the 0.75 CH_4 + 0.25 CO_2, 0.50 CH_4 +0.50 CO_2 and 0.25 CH_4 + 0.75 CO_2 systems, respectively. For all cases, water content in liquid/supercritical phases reduces as temperature decreases, as normally observed in the vapour phase, for instance see Figure 2(f) and 3.

Table 7. Experimental water content at 15 MPa in the carbon dioxide + methane system in equilibrium with hydrates (L: liquid region; SC: supercritical region).

T/ K	Water Content / ppm		
	Z_{CO2} =0.25	Z_{CO2} =0.50	Z_{CO2} =0.75
233.15	11 [SC]	46 [L]	119 [L]
253.15	40 [SC]	98 [L]	286 [L]
263.15	63 [SC]	162 [SC]	417 [L]
268.15	92 [SC]	196 [SC]	534 [L]
273.15	118 [SC]	255 [SC]	663 [L]
278.15	166 [SC]	337 [SC]	794 [L]
288.15	299 [SC]	560 [SC]	1260 [SC]

Comparison between sCPA, SRK-HV-NRTL and EoS-CG predictions and the measurements from Table 7 are depicted in Figure 6 (a)-(c). It is evident that sCPA provides the better representation for water content in liquid and supercritical region. A considerable variation was observed, in terms of absolute average deviations (AAD), between the different equations of state (4, 18 and 49% to sCPA, SRK-HV-NRTL and EoS-CG, respectively).

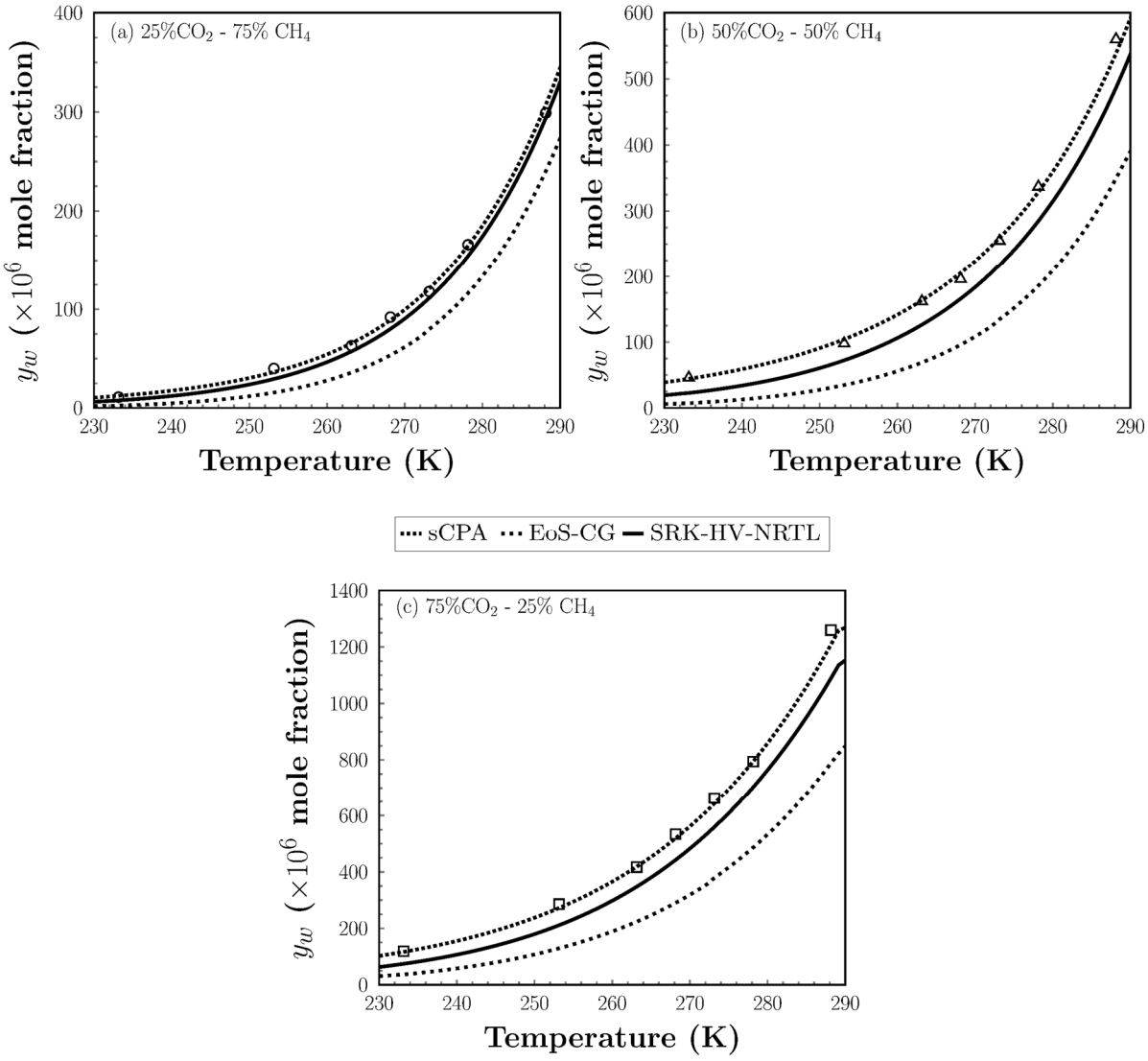

Figure 6. Predictions for water content in carbon dioxide – methane mixtures with different compositions.

It is somewhat surprising that the multiparametric approach yields such poor water content predictions (with AAD = 49%), see dotted lines in Figure 6a-c, although it is regarded as highly accurate in describing natural and combustion gas compounds. Aasen and co-workers also reported lower AAD for a PR-HV-NRTL, in comparison with EoS-CG, in their investigations for CO_2-water mutual solubilities. The authors have attributed this unexpected output to the fact that the multiparametric model was not fitted directly to the selected data used in their work. Moreover, they highlighted that this type of model is normally fitted to more properties than just phase compositions [75].

Given the above, the original GERG-2008 (which includes a binary specific departure function only for carbon dioxide - methane) and EoS-CG predictions were compared, as

given in Figure 7, as a function of initial carbon dioxide concentration. It demonstrated that the combustion gas version only gives good results when $z_{CO_2} \to 0$. In fact, considering the overall CO_2-mole fraction range, GERG-2008 provided better average absolute deviation (23% against 31%). Since EoS-CG includes specific departure functions for water – methane and water – carbon dioxide, this observation was unexpected. This suggests that this multiparametric approach might have limitations in either the specific residual function for carbon dioxide-water or in the mixing rules and extrapolation procedure to multicomponent mixtures.

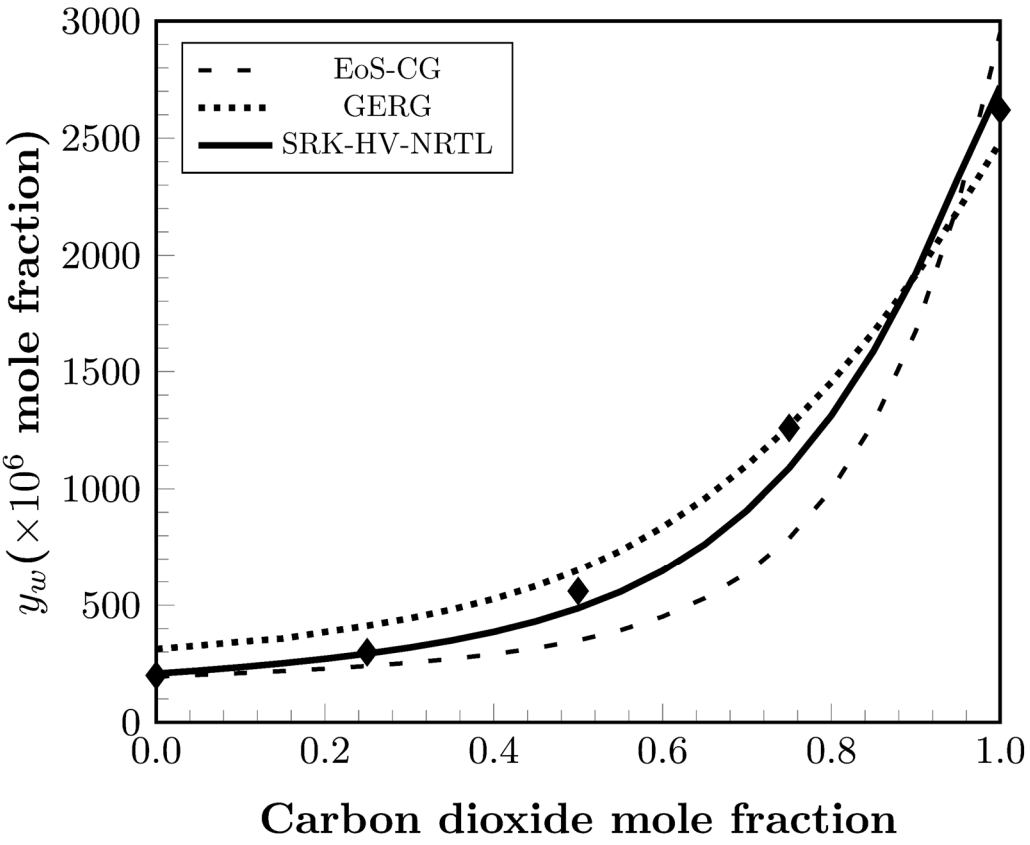

Figure 7. Effect of carbon dioxide content in the water content in the vapour phase at 15 MPa and 288.15K. Measurement for pure carbon dioxide were taken from [72]. Estimation for pure methane is taken from sCPA which fits very well measurements at 288.11K published in [67].

In contrast, SRK – HV – NRTL results are in good agreement with experimental data, although, adherence is better at $z_{CO_2} \leq 0.25$. It might be caused by the limitations described in the adjustment for carbon dioxide – water pair in the vicinity of critical point and supercritical region, see Figure 2d. Regardless the use of only two parameters and the absence of a specific approach to associative molecules, its overall performance can be

considered satisfactory, particularly for those conditions where the model was validated (see previous section).

4.3. Water Content in CO_2-rich mixtures

Measurements have been made for mixtures 1, 2, 3 and 4, for which compositions are given in Table 2, in equilibrium with water or hydrates at a range of temperatures between 233.15 to 288.15 K, at pressures up to 15 MPa. The measurements at lower pressures were made at conditions avoiding coming close to the two-phase region (see Figure 8 and 10 for experimental conditions), except for the measurements undertaken for MIX 4 (see Figure 14).

Table 8 summarises average absolute deviations for each mixture individually. sCPA shows better overall predictions, although SRK-HV-NRTL presented better performance for MIX 2 and 4. Each mixture is briefly discussed in the following sections.

Table 8. Average absolute deviations (ADD) for the models evaluated accounting for each specific mixture. *correspond to the data measured in the liquid vapour region, according to Table 11, for which deviations in the vapour phase at 233.15 K were not considered.

	MIX 1	MIX 2	MIX 3	MIX 4	MIX 4 LV(*)	Average
sCPA	6.0%	10.2%	6.9%	11.8%	12.0%	9.4%
SRK-HV-NRTL	24.2%	4.9%	26.7%	4.9%	13.2%	15.4%
EoS-CG	19.8%	18.4%	20.3%	38.7%	21.6%	23.7%

Mixture 1 (MIX 1): Results for water content in MIX 1 at different temperature and pressures are presented in Table 9. Measurements were carried out in the presence of liquid water or hydrates; T and P condition coordinates are plotted in Figure 8. In addition, Figure 9 compares model predictions and experimental data.

Table 9. Water contents (10^6 mole fraction) for MIX 1 in equilibrium with hydrates or water.

Pressure (MPa)	288.15 K	278.15 K	273.15 K	268.15 K	263.15 K	253.15 K	233.15 K
15	2082	1438	1179	950	763	486	177
10	1945	1388	1134	918	745	477	178
7	-	-	-	882	-	-	-

6	-	-	-	-	715	-	-
5	-	-	-	-	-	464	177

As seen in Figure 9, the water content in MIX 1 is very similar to the behaviour in pure CO_2, however because of the impurities the water content is significantly lower. Consider, for instance, the result at 288.15 K and 15 MPa. When compared with data published by King et al. [55] at very similar conditions, one can conclude that less than 5% impurity content results in an 20% lowering in water concentration in CO_2-rich phase. This finding is in accordance with a previous study [102], and indicates that even a small amount of inert gases might play an important role in water content predictions. Interestingly, these effects have been widely overlooked or even completely ignored, although it might have a considerable impact on dehydration requirements and hydrate prevention (overdesign or underestimation).

Comparing the different modelling approaches, sCPA showed superior capabilities in predicting water content with 6% average deviation. In contrast, EoS-CG and SRK-HV-NRTL basically presented the same deviations (ADD = 20 and 25%, respectively) and were found less accurate, although they can follow the main trend. In general, all the models exhibited higher deviations as temperature decreases.

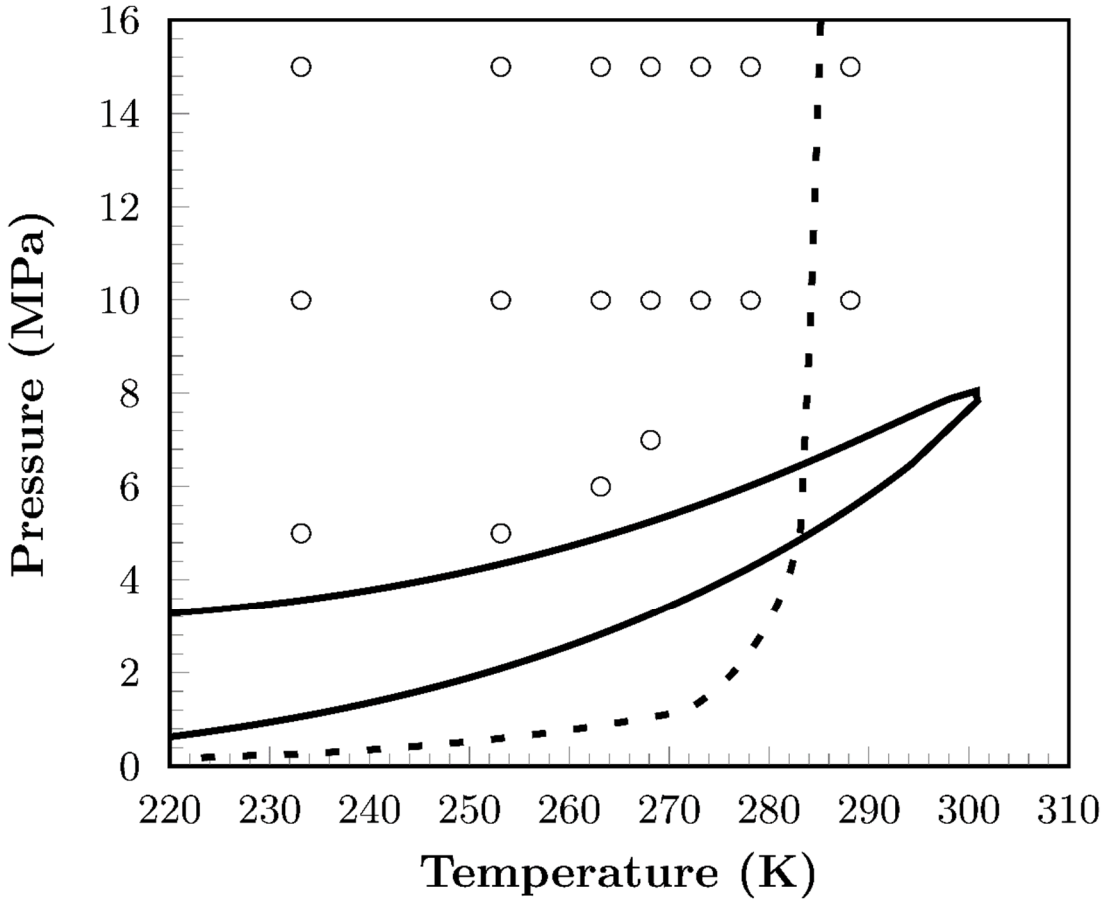

Figure 8. Experimental Conditions for Water Content in MIX 1 in Equilibrium with Hydrates. Marks represent coordinates for data in Table 9 and dashed line, hydrate dissociation conditions.

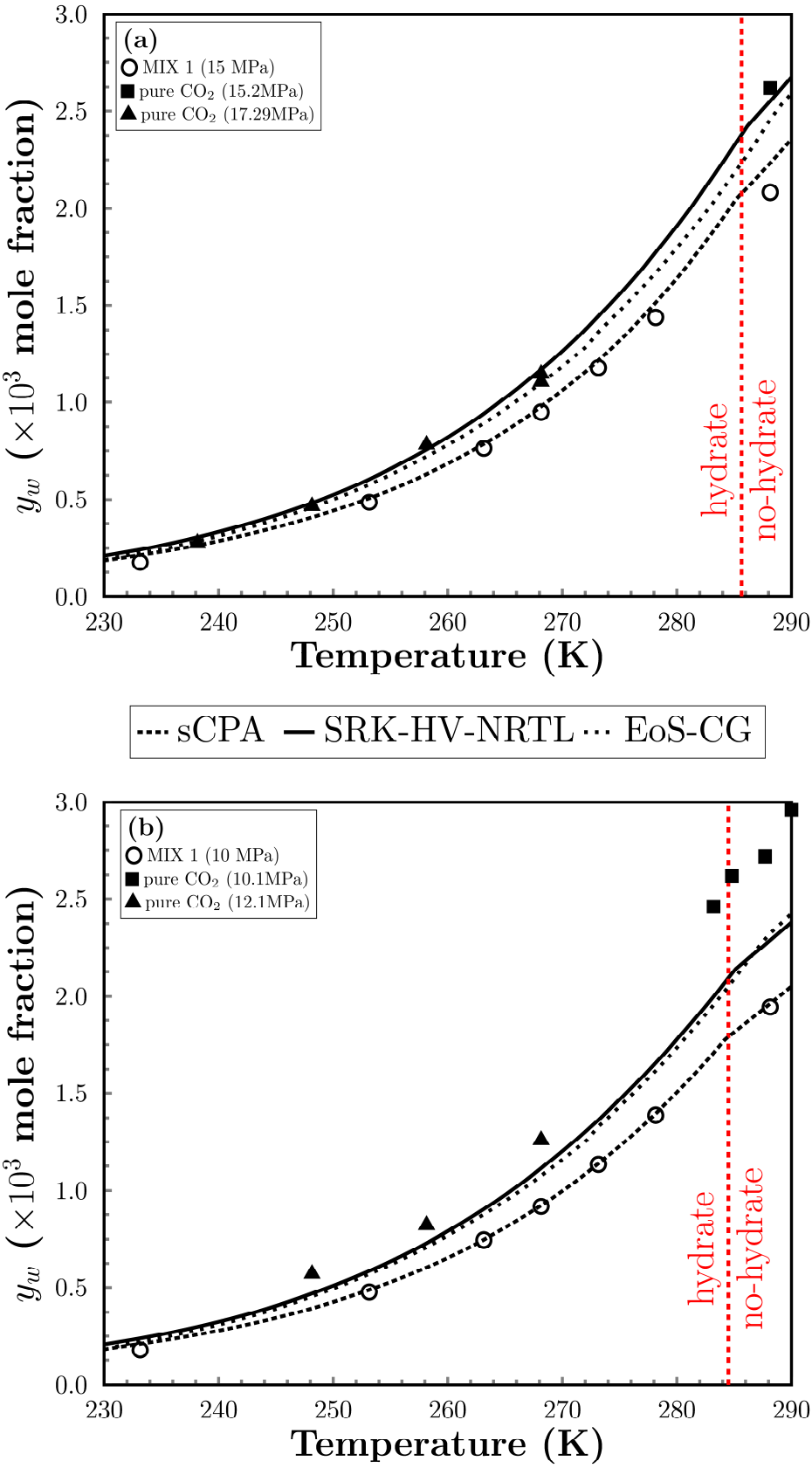

Figure 9. Experimental and predicted water contents (10^6 mole fraction) for pure CO_2 and MIX 1 in equilibrium with hydrates or water. Data for pure CO_2 was taken from King et al. [72] and Jasperson et al. [63].

Mixture 2 (MIX 2): Results for this mixture are presented in Table 9, for which behaviour is more complex, as the water content exhibits a minimum. This characteristic has already been reported for CO_2/methane mixtures by different authors [12,14] and it is attributed to a phase change. Most of the measurements took place in the presence of hydrates, as depicted in Figure 10. Experimental and predicted water content is compared in Figure 11 where the effect of pressure is pointed out.

In this case, SRK-HV-NRTL yields better predictions, with an AAD = 5%, while 10% average deviation was obtained with sCPA. It is also noted that EoS-CG is unable to predict this minimum in pressure. In fact, above 7 MPa, model outcomes exhibited remarkably poor agreement with experimental data, in an almost ideal gas fashion. In spite of this, average deviation maintained the same magnitude observed for the previous mixture, approximately 20%. It is observed that EoS-CG predictions are considerably worse at higher pressures and low temperatures, while the other equations of state compared in this study showed no clear trend.

Table 10. Water contents (10^6 mole fraction) for MIX 2 in equilibrium with hydrates or water.

Pressure (MPa)	288.15K	278.15K	273.15K	268.15K	263.15K	253.15K	233.15K
15	411	239	173	137	102	49	18
10	393	213	151	112	78	38	-
5	523	265	184	119	82	26	-

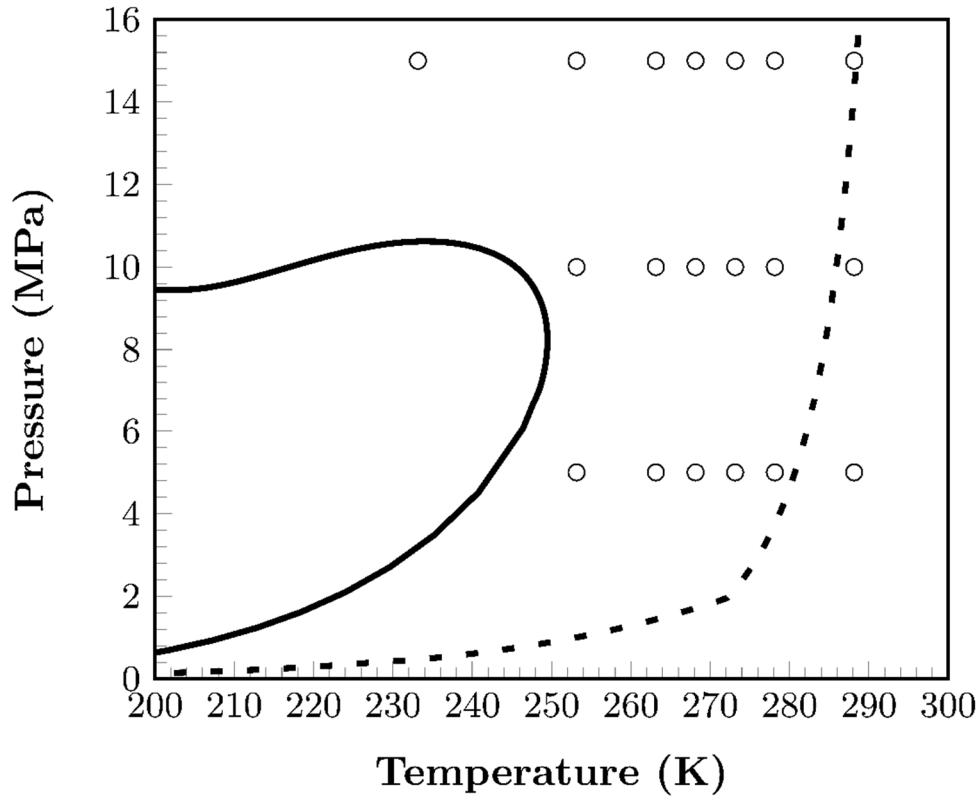

Figure 10. Experimental Conditions for Water Content in MIX 2 in Equilibrium with Hydrates. Marks represent coordinates for data in Table 10 and dashed line, hydrate dissociation conditions.

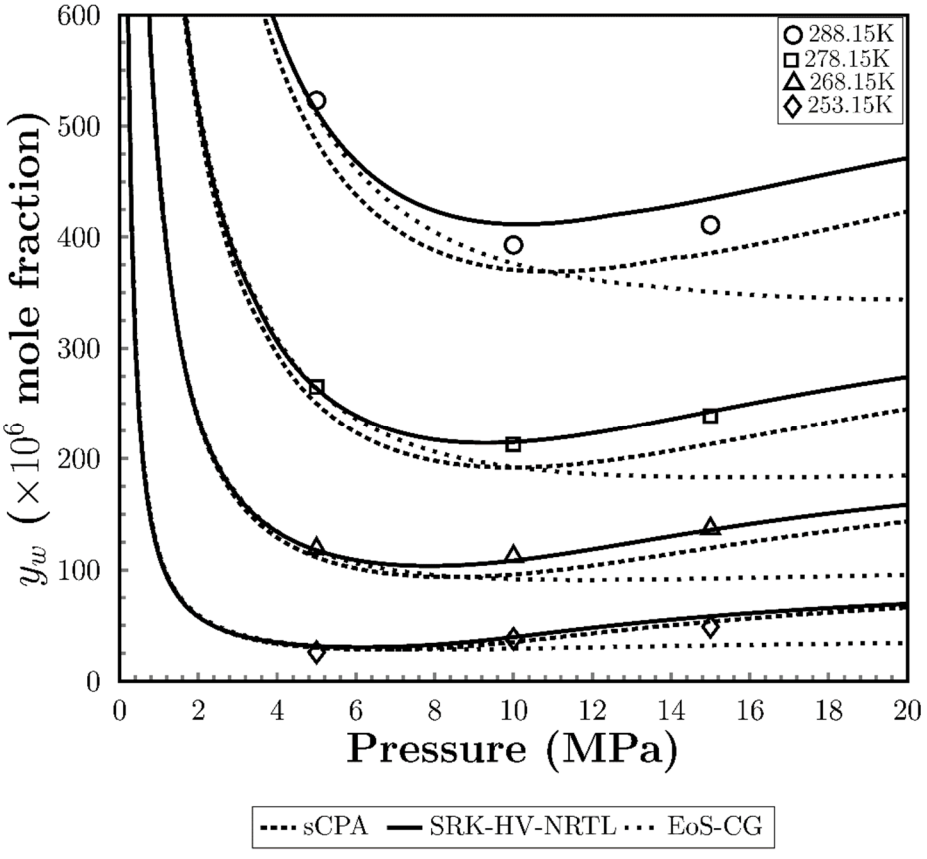

Figure 11. Experimental and predicted water contents (10^6 mole fraction) for MIX 2 in equilibrium with hydrates or water – Pressure effect.

Mixture 3 (MIX 3): Measurements were made at 15 MPa and are presented in Table 11 and compared with predictions in Figure 12. As observed for MIX 1, less than 5% (oxygen, nitrogen, hydrogen and argon) inert gases considerably reduced water content in comparison with pure carbon dioxide. Again, at 288.15 K and 15 MPa, this reduction reached more than 20%. Such results reinforce that small amounts of impurity play an important role in water content for carbon dioxide rich mixtures.

Table 11. Water contents (10^6 mole fraction) for MIX 3 in equilibrium with hydrates or water*

Pressure (MPa)	288.15K	278.15K	273.15K	268.15K	263.15K	253.15K	233.15K
15	2035*	1478	1199	967	781	502	186

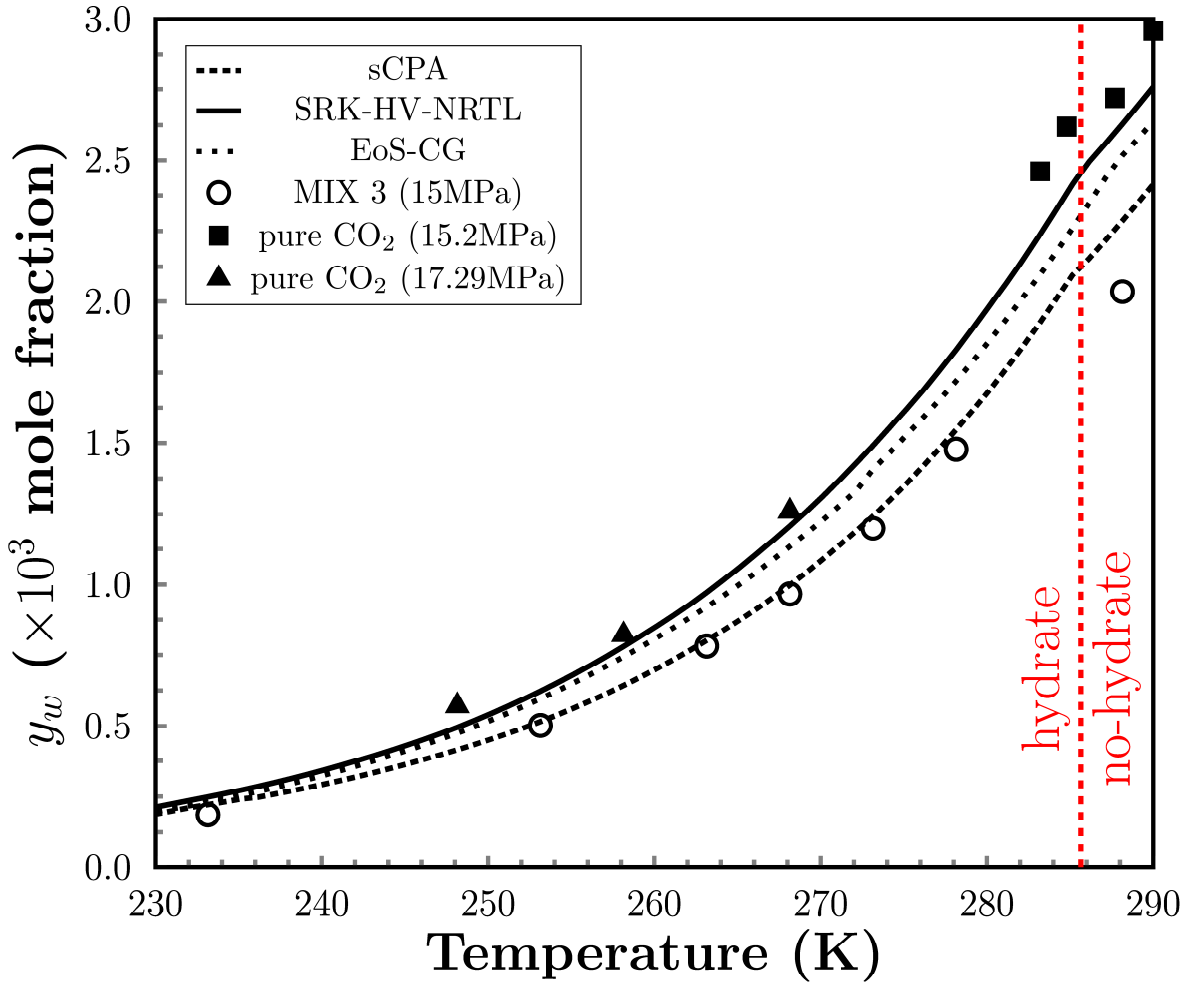

Figure 12. Experimental and predicted water contents (10^6 mole fraction) for MIX 3 in equilibrium with hydrates or water. Data for pure CO_2 was taken from King et al. [72] and Jasperson et al. [63].

Improved predictions for MIX 3 were obtained from sCPA for which ADD was found as low as 7%. Larger deviations were observed for EoS-CG and SRK-HV-NRTL models (20 and 26%, respectively). These values are similar to those achieved for MIX 1.

Mixture 4 (MIX 4): This is a CO_2-rich mixture containing light hydrocarbons, particularly methane, and nitrogen. Results for water content in equilibrium with hydrates or liquid water are shown in Table 12. Experimental data and model predictions are presented in Figure 13. In general, MIX 4 showed the same pattern observed for MIX 1 and 3, regarding the effect of temperature. Moreover, although the mixture has almost 70 % carbon dioxide, reduction in water content, when compared with pure carbon dioxide, corresponds to 60 % at 288.15 K. Again, it highlights the considerable effect of inert gases and hydrocarbons in terms of water content reduction.

Table 12. Water contents (10^6 mole fraction) for MIX 4 in equilibrium with hydrates or water*

Pressure (MPa)	288.15K	278.15K	273.15K	268.15K	263.15K	253.15K	233.15K
15	1037	683	519	399	312	182	68

There was a significant agreement between sCPA and SRK-HV-NRTL predictions and experimental data for MIX 4, see Figure 13. This time, however, the latter showed better results for the whole temperature interval, with ADD = 4.2 %, while the former, 11.8 %. Perhaps the most striking finding was the poor performance of EoS-CG. With the multiparametric model, underestimating predictions with AAD by as much as 38.7 % were observed.

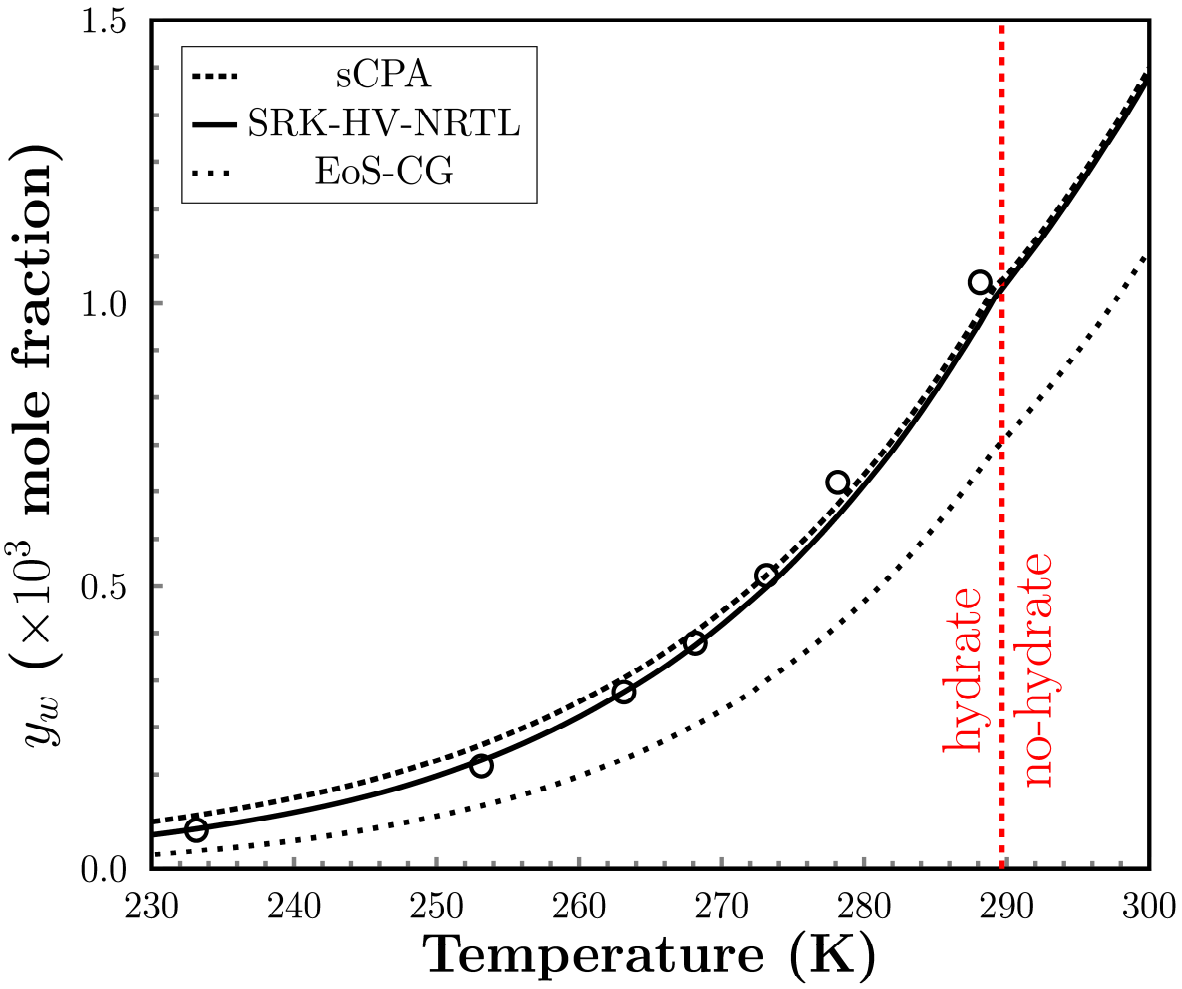

Figure 13. Experimental and predicted water contents (10^6 mole fraction) for MIX 4 in equilibrium with hydrates or water.

For MIX 4 an investigation of water content prediction for vapour-liquid equilibrium in the presence of hydrates was undertaken. To do so, 18 measurements were carried out at temperatures between 233.15 and 263.15 K, and moderate pressures (from 2.8 to 7.7 MPa). The experimental conditions are plotted in Figure 14 and phase compositions are listed in Table 13. To obtain these results, a ratio of 5 cc of water for 295 cc of gas was used in each test.

As observed in Table 13, experiments conducted in the two-phase region produced a CO_2-rich liquid phase (with, at least, 77.6% mole/mole), containing between 102 and 640 ppmV of water (moles/10^6 mole), and a vapour phase containing mainly methane and carbon dioxide and up to 100 ppmV of water vapour.

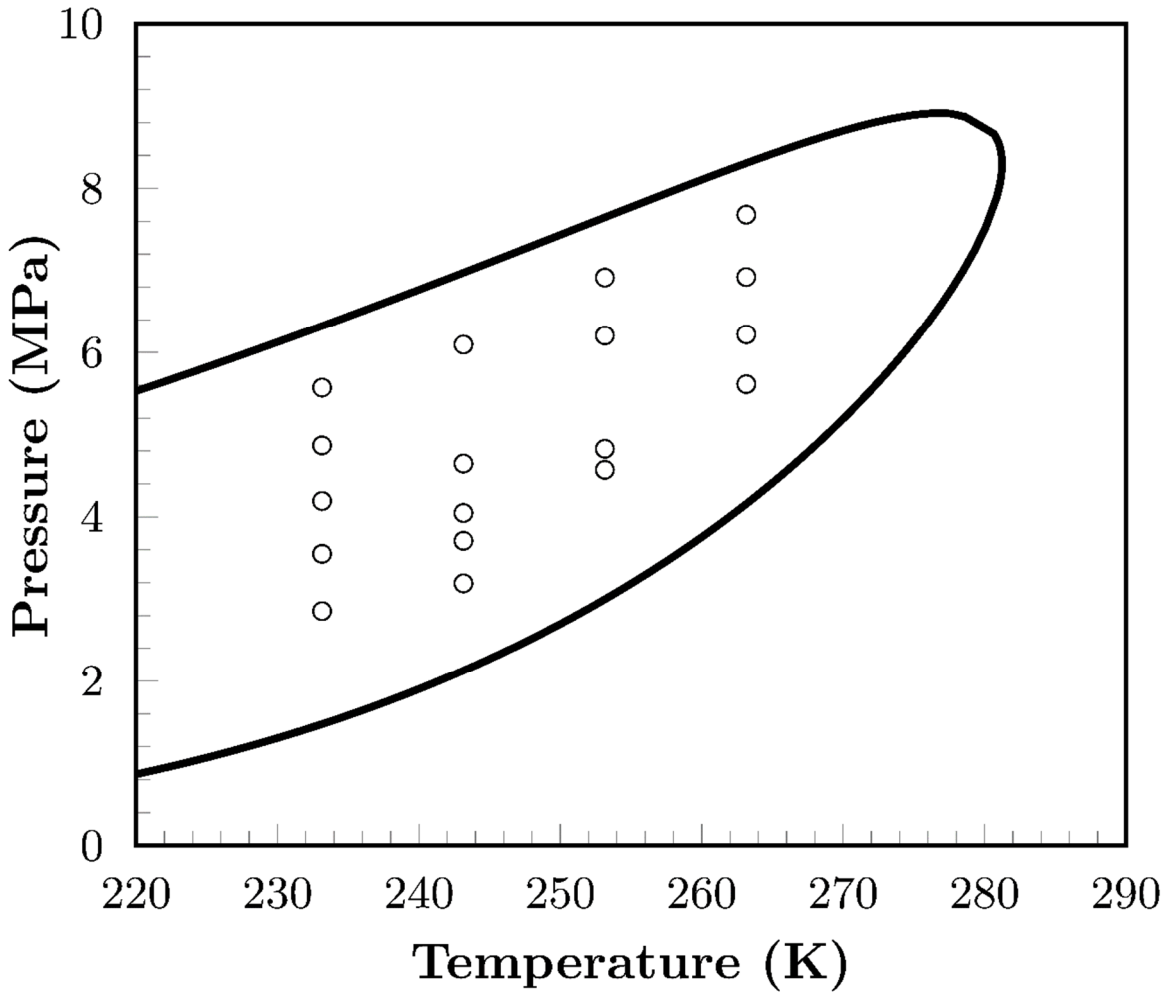

Figure 14. Experimental Conditions for Water Content in MIX 4 in Equilibrium with Hydrates within the 2-phases region. Marks represent coordinates for data in Table 13.

Table 13. Water content (Y_w, in ppm, 10^6 mole fraction) and composition of vapour and liquid phases in equilibrium with hydrates for tests with MIX 4. L and V referred to Liquid and Vapour phase, respectively.

	T (K)	P (MPa)	C1	C2	C3	iC4	NC4	iC5	CO_2	N_2	nC5	Y_w
L	263.15	5.61	9.5667%	0.9313%	0.4824%	0.1430%	0.1421%	0.0855%	87.7951%	0.7945%	0.0594%	540
L	263.15	6.22	14.9786%	0.9408%	0.4080%	0.1099%	0.1093%	0.0631%	82.0490%	1.2982%	0.0431%	611
L	263.15	6.92	14.4525%	0.9564%	0.4014%	0.1042%	0.1021%	0.0560%	82.5744%	1.3137%	0.0394%	495
L	263.15	7.68	19.3672%	0.9625%	0.3556%	0.0869%	0.0842%	0.0498%	77.5854%	1.4752%	0.0332%	431
L	253.15	4.57	6.8840%	0.9038%	0.4707%	0.1357%	0.1347%	0.0797%	90.9849%	0.3496%	0.0569%	431
L	253.15	4.83	8.5730%	0.8340%	0.4048%	0.1123%	0.1131%	0.0658%	89.2504%	0.5989%	0.0477%	379
L	253.15	6.21	12.3726%	0.8931%	0.3589%	0.0873%	0.0846%	0.0465%	85.2942%	0.8324%	0.0302%	302
L	253.15	6.92	18.5888%	0.9637%	0.3516%	0.0831%	0.0794%	0.0398%	78.4043%	1.4608%	0.0286%	223
L	243.15	3.19	2.3100%	0.7402%	0.4857%	0.1594%	0.1620%	0.1023%	95.7873%	0.1769%	0.0762%	325
L	243.15	3.71	2.9478%	0.7635%	0.4528%	0.1380%	0.1378%	0.0887%	95.2671%	0.1470%	0.0572%	272
L	243.15	4.05	7.0767%	0.8454%	0.3969%	0.1048%	0.1022%	0.0606%	90.9390%	0.4353%	0.0391%	240
L	243.15	4.65	6.7164%	0.8642%	0.4150%	0.1155%	0.1130%	0.0714%	91.1489%	0.5119%	0.0437%	226
L	243.15	6.09	11.4650%	0.8904%	0.3616%	0.0929%	0.0911%	0.0523%	86.4211%	0.5902%	0.0355%	223
L	233.15	2.85	1.5434%	0.8129%	0.4663%	0.1298%	0.1335%	0.0945%	96.6082%	0.1415%	0.0700%	172
L	233.15	3.55	5.0441%	0.9558%	0.4653%	0.1253%	0.1224%	0.0703%	92.9116%	0.2555%	0.0497%	148
L	233.15	4.19	6.4868%	0.9690%	0.4487%	0.1178%	0.1179%	0.0677%	91.3765%	0.3694%	0.0462%	133
L	233.15	4.87	13.3769%	1.0311%	0.4041%	0.0924%	0.0924%	0.0509%	84.2612%	0.6567%	0.0343%	120
L	233.15	5.57	12.1038%	0.9763%	0.3895%	0.0977%	0.0988%	0.0588%	85.6525%	0.5825%	0.0400%	102

V	263.15	5.61	43.875%	0.912%	0.163%	0.020%	0.015%	0.005%	49.701%	5.309%	0.002%	87
V	263.15	6.22	49.418%	0.857%	0.128%	0.016%	0.013%	0.007%	43.658%	5.899%	0.004%	96
V	263.15	6.92	50.217%	0.842%	0.122%	0.013%	0.010%	0.006%	42.410%	6.377%	0.003%	92
V	263.15	7.68	54.373%	0.778%	0.108%	0.012%	0.010%	0.003%	37.780%	6.933%	0.002%	96
V	253.15	4.57	57.824%	0.704%	0.094%	0.011%	0.008%	0.003%	33.397%	7.957%	0.002%	38
V	253.15	4.83	50.077%	0.767%	0.122%	0.015%	0.012%	0.005%	42.475%	6.524%	0.003%	35
V	253.15	6.21	45.183%	0.840%	0.141%	0.017%	0.013%	0.005%	48.212%	5.586%	0.003%	33
V	253.15	6.92	46.163%	0.920%	0.158%	0.019%	0.015%	0.005%	47.627%	5.091%	0.003%	33
V	243.15	3.19	53.049%	0.784%	0.129%	0.018%	0.015%	0.005%	39.087%	6.909%	0.003%	15
V	243.15	3.71	44.626%	0.842%	0.169%	0.026%	0.023%	0.008%	49.033%	5.267%	0.006%	16
V	243.15	4.05	44.884%	0.821%	0.167%	0.026%	0.023%	0.010%	48.376%	5.686%	0.007%	10
V	243.15	4.65	40.028%	0.911%	0.201%	0.032%	0.027%	0.010%	53.811%	4.973%	0.006%	11
V	243.15	6.09	42.233%	0.884%	0.178%	0.026%	0.022%	0.007%	51.688%	4.956%	0.005%	12
V	233.15	2.85	54.481%	0.956%	0.124%	0.012%	0.008%	0.003%	38.253%	6.161%	0.002%	2
V	233.15	3.55	59.642%	0.869%	0.106%	0.010%	0.008%	0.002%	32.379%	6.983%	0.002%	2
V	233.15	4.19	62.415%	0.796%	0.092%	0.009%	0.007%	0.002%	28.992%	7.686%	0.002%	1
V	233.15	4.87	64.098%	0.729%	0.084%	0.008%	0.007%	0.002%	26.603%	8.467%	0.001%	2
V	233.15	5.57	65.117%	0.685%	0.077%	0.008%	0.006%	0.002%	24.914%	9.189%	0.001%	4

Figure 15 compares experimental and predicted values for the data displayed in Table 8. Overall, the three different models are predicting the compositions in all phase with the correct trend of changes. The CPA method showed the best agreement between predictions and experimental results, particularly in the vapour phase. SRK-HV-NRTL yielded larger deviations, although, for many conditions, it reproduces sCPA results and tendencies.

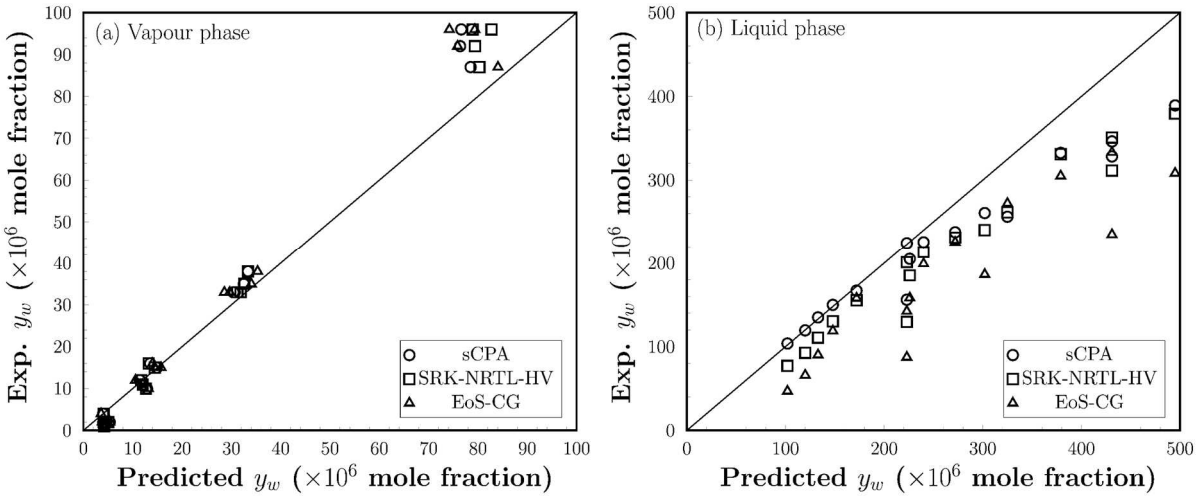

Figure 15. Comparative between experimental and predicted water content, data presented in Table 13.

Underprediction was observed for water content in the liquid phase, no matter the approach used, although, it was more evident for EoS-CG model. Interestingly, sCPA provided accurate predictions in liquid phase for 233.15 K.

Overall models evaluation: The present analysis highlights the importance of investigating capabilities and limitations of equations of state in extrapolating predictions to multicomponent mixtures. For instance, the accurate multiparametric EoS-CG/GERG approach showed severe limitations and a massive downgrade in accuracy when used with methane/carbon dioxide or CO_2-rich multicomponent mixtures with water. It shows how complex is the task of extending the models based on parameters fitted from binary systems to complex multicomponent ones. Considering the unexpectedly high average deviations (50% for the ternary mixture and 27% for MIX 1 to 4), it was also observed that EoS-CG performed better when dealing with MIX 1 and 3 (z_{CO2} > 95%), and, when $z_{CO2} \rightarrow 0$, in the case of $CO_2/CH_4/H_2O$ (Figure 7). Moreover, the original GERG-2008 (which includes binary specific departure function only for carbon dioxide - methane) provided better average absolute deviation (23% against 31%) than EoS-CG (which includes specific

departure functions for water – methane and water – carbon dioxide). The most intriguing fact is that this model performs more satisfactorily when there is a major component for which $x_i \rightarrow 1$. Thus, it is possible that, for GERG multiparametric approach, the applied mixing rules are unable to conserve main features from the specific binary functions when extending the approach to multicomponent systems.

On the contrary, sCPA has demonstrated a good ability to deal with water containing CO_2-rich systems, within the scope of this study. Although, it exhibited lower accuracy for MIX 2 and MIX 4 and at very low temperatures, its overall predictions can be considered satisfactory.

SRK-HV-NRTL showed better results when Huron-Vidal approach was applied only to water – carbon dioxide and water – methane. It suggests that the simpler, the better in incorporating NRTL to SRK. In general, SRK-HV-NRTL model is unable to reproduce the same overall accuracy as sCPA, although, considering the use of only two parameters, it displayed impressive predictive abilities. Particularly for those multicomponent mixtures with initial composition closer to equimolar CO_2/CH_4 (MIX 2 and 4), Huron-Vidal has yielded the best results.

In summary, the cubic-plus association version of SRK (previously evaluated for methane-water and carbon dioxide – water binary systems, and that has showed satisfactory water content prediction capabilities [20,32,103–105]) was found to be the the only model, among those considered in this study, capable of satisfactorily predict water content on CO_2-CH_4 and CO_2-rich multicomponent, at temperatures between 233.15 and 288.15K and pressures up to 15 MPa, which also include equilibrium conditions with hydrates. It was observed that sCPA was also able to deal with the effect of common impurities, particularly at low concentration, on the water content, as considerable reductions compared with pure carbon dioxide was observed.

5. Conclusion

An experimental and modelling study of CO_2-rich mixtures with water was performed for temperatures between 233.15 and 288.15 K and pressures up to 15 MPa. This included

equilibrium between hydrates or liquid water with liquid or vapour methane/carbon dioxide or CO_2-rich mixtures containing light hydrocarbons (Methane, Ethane, Propane, n- Butane, i-Butane, n-Pentane and I-Pentane) and inert gases (Nitrogen, Hydrogen and Argon). In addition, water content measurements inside the two-phase region in the presence of hydrates were carried out. Complete composition for liquid and vapour phases were reported.

Focusing on industrial applications, the capabilities and limitations of three different equation of state approaches (association model theory, Gibbs excess energy model coupling with cubic equations of state and highly accurate multiparametric GERG) were undertaken. Evaluations were focused on water content predictions for CO_2-rich fluid phases. From this work, it can be concluded that:

- In the application of a SRK-HV-NRTL model fitted from binary systems data, the best results were obtained when Huron-Vidal mixing rules were limited to methane – water and carbon dioxide – water parameters.

- Small amounts of inert gases in rich-CO_2 streams resulted in a considerable reduction in water content in the fluid phases. It was found that less than 5% permanent gases in initial composition resulted in a 20% water concentration reduction at 288.15 K and 15 MPa. A similar tendency was observed when hydrocarbons are present (92%, 81 % and 55% average reduction compared to pure CO_2 in the 0.75 CH_4 + 0.25 CO_2, 0.50 CH_4 +0.50 CO_2 and 0.25 CH_4 + 0.75 CO_2 systems, respectively). These results are somewhat counterintuitive and indicate that, although very tempting, approximate CO_2-rich mixtures (even when Z_{CO2} > 95%) to pure carbon dioxide will lead to considerable water content overestimations (and all the consequent implications such as overdesign, hydrates inhibitors overdosage, etc…).

- Although regarded as a highly accurate model, EoS-CG/GERG approach has been found very limited when dealing with water plus CO_2/CH_4 or CO_2-rich-mixtures. In

fact, no AAD lower than 18% could be found in any studied case. Considering the unexpectedly high average deviations (49% for the ternary mixture and 23.7% for MIX 1 to 4), it was also observed that EoS-CG performed better when dealing with MIX 1 and 3 (z_{CO2} > 95%), and, when $z_{CO2} \rightarrow 0$, in the case of $CO_2/CH_4/H_2O$. Thus, it is possible that, for GERG multiparametric approach, the applied mixing rules are unable to conserve the main features from the specific binary functions when extrapolated to multicomponent systems.

- For the CO_2-rich mixtures studied in this work, sCPA exhibited overall better predictions and lower average absolute deviations. For the specific case of MIX 2 and 4, SRK-HV-NRTL showed slightly better results. Considering that Huron-Vidal approach used only two parameters, these were considered impressive predictive abilities.

- In addition, water content measurements were carried out in two phase-region in the presence of hydrates. Composition of liquid and vapour phases were also reported. Despite the overall satisfactory agreement, underpredicted results were observed for water content in the liquid phase, no matter the approach used (although, it was more evident for EoS-CG model).

Acknowledgement

Work presented in this paper was conducted in support of projects funded by Galp Energia, Linde AG, Petrobras, Petronas, Equinor and Total which is gratefully acknowledged.

Valderio de O. Cavalcanti Filho acknowledges the financial support from Petrobras through his PhD Grant.

Abbreviations

AAD	Average absolute deviation
BIP	Binary Interaction Parameters
CCS	Carbon capture and storage
CR-1	Combining Rule for association parameters
EOR	Enhanced oil recovery
EoS	Equation of State
EoS-CG	Combustion Gas Equation of State
FID	Flame Ionisation Detector
GERG	The European Gas Research Group
HV	Huron-Vidal EoS/G^{ex} mixing rule
L	Liquid Phase
L_w	Liquid aqueous phase
L_{CO2}	Liquid carbon dioxide-rich phase
NAMAS	National Measurement Accreditation Service
NRTL	Non-random two-liquid
PC-SAFT	Perturbated Chain Statistical Association Theory
PR	Peng-Robinson
PRSV	Peng–Robinson–Stryjek–Vera
PTR	Platinum Resistance Thermometer
PR-UMR	Peng-Robinson Universal Mixing Rules
SAFT	Statistical Association Fluid Theory
SAFT-VR	Variable Range Statistical Association Fluid Theory
SC	Supercritical
sCPA	Simplified Cubic-Plus Association
SRK	Soave-Redlich-Kwong
TCD	Thermal Conductive Detector
TDLAS	Tunable diode laser absorption spectroscopy
V	Vapour Phase
VLE	Vapor-Liquid Equilibrium
VLLE	Vapor-Liquid-Liquid Equilibrium
VTPR	Volume Translated Peng-Robinson
WAG	Water alternated gas
WS	Wong-Sandler EoS/Gex mixing rule

Nomenclature

a	Mixture attractive parameter for cubic EoS
a_i	Pure component attraction parameter for Cubic EoS
b	Mixture Co-volume
b_i	Pure component co-volume
c_1, c_2, c_3	coefficients for Mathias-Copeman alpha function
F_{ij}	Binary coefficient for departure functions for GERG/EoS-CG
G^{ex}	Gibbs excess energy
P	Pressure
v	Molar volume
R	Universal gas constant
T	Temperature
g	Radial distribution function (RDF) for sCPA
x_i	Mole fraction of component i
X^{ai}	Fraction of non-bonded components at site Ai
z_i	Initial mole fraction of component i

Greek Symbols

α	Dimensionless Helmholtz energy

$\alpha(T)$	Alpha function for SRK and PR EoS
α_{ij}	Non-randomness parameter between component i and j in NRTL Gibbs excess model
β^{AiBj}	Association volume parameter between sites Ai and Bj used in sCPA
Δ^{AiBj}	Strength of interaction between sites Ai and Bj used in sCPA
$\beta_{v,ij}$ $\beta_{T,ij}$	Adjustable parameters for GERG and EoS-CG equations
δ	Reduced mixture density used in GERG and EoS-CG models
ε^{ij}	Association energy between sites Ai and Bj used in sCPA model
ρ	Molar density
$\gamma_{v,ij}$ $\gamma_{T,ij}$	Adjustable parameters for GERG and EoS-CG equations
τ	Reduced mixture temperature used in GERG and EoS-CG models
τ_{ij}, τ_{ji}	Parameters for NRTL model

References

[1] J.J. Carrol, Natural Gas Hydrates - A Guide for Engineers, Gulf Professional Publishing, 2009. https://doi.org/https://doi.org/10.1016/B978-0-7506-8490-3.X0001-8.

[2] A.M.T. De Andrade, C.E.M. Vaz, J. Ribeiro, L.G.R. Lopreato, R.F.S. do Nascimento, Offshore Production Units for Pre-Salt Projects, Offshore Technol. Conf. (2015).

[3] A. Chapoy, R. Burgass, A. Terrigeol, C. Coquelet, A.T.C.C. Antonin Chapoy Rod Burgass, A. Chapoy, R. Burgass, A. Terrigeol, C. Coquelet, Water Content of CO 2 -rich Mixtures: Measurements and Modeling using the Cubic-Plus-Association Equation of State , J. Nat. Gas Eng. 1 (2016) 85–97. https://doi.org/10.7569/jnge.2015.692505.

[4] A. Dhima, J.C. De Hemptinne, J. Jose, Solubility of hydrocarbons and CO2 mixtures in water under high pressure, Ind. Eng. Chem. Res. 38 (1999) 3144–3161. https://doi.org/10.1021/ie980768g.

[5] Y. Bi, T. Yang, K. Guo, Determination of the upper-quadruple-phase equilibrium region for carbon dioxide and methane mixed gas hydrates, J. Pet. Sci. Eng. (2013). https://doi.org/10.1016/j.petrol.2012.11.019.

[6] P. Kastanidis, G.E. Romanos, A.K. Stubos, I.G. Economou, I.N. Tsimpanogiannis, Two- and three-phase equilibrium experimental measurements for the ternary CH4 + CO2 + H2O mixture, Fluid Phase Equilib. 451 (2017) 96–105. https://doi.org/10.1016/j.fluid.2017.08.002.

[7] J.H. Erbar, A.K. Jagota, S. Muthswamy, M. Mosheghian, Prediction stnthetic gas and natural gas thermodynamic properties using a modified Soave-Redlich-Kwong equation of state, Tulsa, 1980.

[8] P. Kastanidis, V.K. Michalis, G.E. Romanos, A.K. Stubos, I.G. Economou, I.N. Tsimpanogiannis, Solubility of Methane and Carbon Dioxide in the Aqueous Phase of the Ternary (Methane + Carbon Dioxide + Water) Mixture: Experimental Measurements and Molecular Dynamics Simulations, J. Chem. Eng. Data. 63 (2018) 1027–1035. https://doi.org/10.1021/acs.jced.7b00777.

[9] L.N. Legoix, L. Ruffine, J.P. Donval, M. Haeckel, Phase equilibria of the CH4-CO2 binary and the CH4-CO2-H2O ternary mixtures in the presence of a CO2-rich liquid phase, Energies. (2017). https://doi.org/10.3390/en10122034.

[10] K. Ohgaki, K. Takano, H. Sangawa, T. Matsubara, S. Nakano, Methane exploitation by carbon dioxide from gas hydrates - Phase equilibria for CO2-CH4 mixed hydrate system, J. Chem. Eng. Japan. (1996). https://doi.org/10.1252/jcej.29.478.

[11] J. Qin, R.J. Rosenbauer, Z. Duan, Experimental Measurements of Vapor–Liquid Equilibria of the H2O + CO2 + CH4 Ternary System, J. Chem. Eng. Data. 53 (2008) 1246–1249. https://doi.org/10.1021/je700473e.
[12] K.Y. Song, R. Kobayashi, The Water Content of a CO2-Rich Gas Mixture Containing 5.31 mol % Methane along the Three-Phase and Supercritical Conditions, J. Chem. Eng. Data. 35 (1990) 320–322. https://doi.org/10.1021/je00061a026.
[13] C. Jarne, S.T. Blanco, M.A. Gallardo, E. Rauzy, S. Otín, I. Velasco, Dew points of ternary methane (or ethane) + carbon dioxide + water mixtures: Measurement and correlation, Energy and Fuels. 18 (2004) 396–404. https://doi.org/10.1021/ef030146u.
[14] W.A. Fouad, M. Yarrison, K.Y. Song, K.R. Cox, W.G. Chapman, High pressure measurements and molecular modeling of the water content of acid gas containing mixtures, AIChE J. 61 (n.d.) 3038–3052. https://doi.org/10.1002/aic.14885.
[15] S.Z.S. Al Ghafri, E. Forte, G.C. Maitland, J.J. Rodriguez-Henríquez, J.P.M. Trusler, Experimental and Modeling Study of the Phase Behavior of (Methane + CO2 + Water) Mixtures, J. Phys. Chem. B. 118 (2014) 14461–14478. https://doi.org/10.1021/jp509678g.
[16] V. Belandria, A. Eslamimanesh, A.H. Mohammadi, P. Théveneau, H. Legendre, D. Richon, Compositional analysis and hydrate dissociation conditions measurements for carbon dioxide + methane + water system, Ind. Eng. Chem. Res. 50 (2011) 5783–5794. https://doi.org/10.1021/ie101959t.
[17] Y.T. Seo, H. Lee, J.H. Yoon, Hydrate phase equilibria of the carbon dioxide, methane, and water system, J. Chem. Eng. Data. 46 (2001) 381–384. https://doi.org/10.1021/je000237a.
[18] H. Bruusgaard, J.G. Beltrán, P. Servio, Solubility measurements for the CH4 + CO2 + H2O system under hydrate-liquid-vapor equilibrium, Fluid Phase Equilib. 296 (2010) 106–109. https://doi.org/10.1016/j.fluid.2010.02.042.
[19] Y.T. Seo, H. Lee, Multiple-phase hydrate equilibria of the ternary carbon dioxide, methane, and water mixtures, J. Phys. Chem. B. 105 (2001) 10084–10090. https://doi.org/10.1021/jp011095+.
[20] A. Chapoy, H. Haghighi, R. Burgass, B. Tohidi, Gas hydrates in low water content gases: Experimental measurements and modelling using the CPA equation of state, Fluid Phase Equilib. 296 (2010) 9–14. https://doi.org/https://doi.org/10.1016/j.fluid.2009.11.026.
[21] A. Chapoy, H. Haghighi, R. Brugrass, B. Tohidi, On the phase behaviour of the (carbon dioxide + water) system at low temperatures: Experimental and modeling, J. Chem. Eng. 47 (2012) 6–12.
[22] L. V. Jasperson, J.W. Kang, C.S. Lee, D. MacKlin, P.M. Mathias, R.J. McDougal, W.G. Rho, D. Vonniederhausern, Experimental Determination of the Equilibrium Water Content of CO<inf>2</inf> at High Pressure and Low Temperature, J. Chem. Eng. Data. 60 (2015) 2674–2683. https://doi.org/10.1021/acs.jced.5b00320.
[23] G.K. Folas, E.W. Froyna, J. Lovland, G.M. Kontogeorgis, E. Solbraa, Data and prediction of water content of high pressure nitrogen, methane and natural gas, Fluid Phase Equilib. 252 (2007) 162–174. https://doi.org/https://doi.org/10.1016/j.fluid.2006.12.018.
[24] A. Chapoy, C. Coquelet, D. Richon, Solubility measurement and modeling of water in the gas phase of the methane/water binary system at temperatures from 283.08 to

318.12K and pressures up to 34.5MPa, Fluid Phase Equilib. 214 (2003) 101–117. https://doi.org/https://doi.org/10.1016/S0378-3812(03)00322-4.
[25] K.Y. Song, R. Kobayashi, Water Content of CO2 in Equilibrium with Liquid Water and/or Hydrates, SPE Form. Eval. 2 (1987) 500–508.
[26] H.G. Donnelly, D.L. Katz, Phase Equilibria in the Carbon Dioxide–Methane System, Ind. Eng. Chem. (1954). https://doi.org/10.1021/ie50531a036.
[27] R. Wiebe, V.L. Gaddy, Vapor Phase Composition of Carbon Dioxide-Water Mixtures at Various Temperatures and at Pressures to 700 Atmospheres, J. Am. Chem. Soc. 63 (1941) 475–477. https://doi.org/10.1021/ja01847a030.
[28] A.D. King, C.R. Coan, Solubility of water in compressed carbon dioxide, nitrous oxide, and ethane. Evidence for hydration of carbon dioxide and nitrous oxide in the gas phase, J. Am. Chem. Soc. 93 (1971) 1857–1862. https://doi.org/10.1021/ja00737a004.
[29] P.C. Gillespie, G.M. Wilson, GPA Research Report: Vapor-Liquid and Liquid-Liquid Equilibria: Water - Methane, Water - Carbon Dioxide, Water - Hydrogen Sulfide, Water - n-Pentane, Water - Methane - n-Pentane, 1982.
[30] K. Ohgaki, M. Nishikawa, T. Furuichi, T. Katayama, Entrainer Effect of H2O and Ethanol on alpha-Tocopherol Extraction by Compressed CO2, Kagaku Kogaku Ronbunshu. (1988).
[31] T. Nakayama, H. Sagara, K. Arai, S. Saito, High pressure liquid-liquid equilibria for the system of water, ethanol and 1,1-difluoroethane at 323.2 K, Fluid Phase Equilib. 38 (1987) 109–127. https://doi.org/https://doi.org/10.1016/0378-3812(87)90007-0.
[32] R. Burgass, A. Chapoy, P. Duchet-Suchaux, B. Tohidi, Experimental water content measurements of carbon dioxide in equilibrium with hydrates at (223.15 to 263.15)K and (1.0 to 10.0)MPa, J. Chem. Thermodyn. 69 (2014) 1–5. https://doi.org/https://doi.org/10.1016/j.jct.2013.09.033.
[33] J.A. Briones, J.C. Mullins, M.C. Thies, B.-U. Kim, Ternary phase equilibria for acetic acid-water mixtures with supercritical carbon dioxide, Fluid Phase Equilib. 36 (1987) 235–246. https://doi.org/https://doi.org/10.1016/0378-3812(87)85026-4.
[34] I.P. Sidorov, Y.S. Kazarnovskii, A.M. Goldman, The Solubility of Water in compressed Gases, Tr. Gos. Nauchno Issled. Proektn. Inst. Azotn. Promst. Prod. Org. Sin. 1 (1953) 48–67.
[35] R.D. Smith, H.R. Udseth, B.W. Wright, Micro-scale methods for characterization of supercritical fluid extraction and fractionation processes, Process Technol. Proc. 3 (1985) 191–223.
[36] G. Mueller, phd. thesis, Univ. Kaiserslautern, 1983.
[37] J.A. Nighswander, N. Kalogerakis, A.K. Mehrotra, Solubilities of Carbon Dioxide in Water and 1 Wt % NaCl Solution At Pressures up to 10 MPa and Temperatures from 80 to 200 °C, J. Chem. Eng. Data. (1989). https://doi.org/10.1021/je00057a027.
[38] A. Bamberger, G. Sieder, G. Maurer, High-pressure (vapor+liquid) equilibrium in binary mixtures of (carbon dioxide+water or acetic acid) at temperatures from 313 to 353 K, J. Supercrit. Fluids. 17 (2000) 97–110. https://doi.org/https://doi.org/10.1016/S0896-8446(99)00054-6.
[39] D.-Q.Q. Zheng, W.-D.D. Ma, R. Wei, T.-M.M. Guo, Solubility study of methane, carbon dioxide and nitrogen in ethylene glycol at elevated temperatures and pressures, Fluid Phase Equilib. 155 (1999) 277–286. https://doi.org/https://doi.org/10.1016/S0378-3812(98)00469-5.

[40] C.F. Prutton, R.L. Savage, The Solubility of Carbon Dioxide in Calcium Chloride-Water Solutions at 75, 100, 120° and High Pressures, J. Am. Chem. Soc. (1945). https://doi.org/10.1021/ja01225a047.
[41] J. Kiepe, S. Horstmann, K. Fischer, J. Gmehling, Experimental determination and prediction of gas solubility data for CO2 + H2O mixtures containing NACl or KCl at temperatures between 313 and 393 K and pressures up to 10 MPa, Ind. Eng. Chem. Res. (2002). https://doi.org/10.1021/ie020154i.
[42] D.Q. Zheng, T.M. Guo, H. Knapp, Experimental and modeling studies on the solubility of CO2, CHClF2, CHF3, C2H2F4 and C2H4F2 in water and aqueous NaCl solutions under low pressures, Fluid Phase Equilib. (1997). https://doi.org/10.1016/s0378-3812(96)03177-9.
[43] M.S.-W. Wei, T.S. Brown, A.J. Kidnay, E.D. Sloan, Vapor + Liquid Equilibria for the Ternary System Methane + Ethane + Carbon Dioxide at 230 K and Its Constituent Binaries at Temperatures from 207 to 270 K, J. Chem. Eng. Data. 40 (1995) 726–731. https://doi.org/10.1021/je00020a002.
[44] S. Bando, F. Takemura, M. Nishio, E. Hihara, M. Akai, Solubility of CO2 in aqueous solutions of NaCl at (30 to 60)°C and (10 to 20) MPa, J. Chem. Eng. Data. (2003). https://doi.org/10.1021/je0255832.
[45] L. Ruffine, J.P.M. Trusler, Phase behaviour of mixed-gas hydrate systems containing carbon dioxide, J. Chem. Thermodyn. (2010). https://doi.org/10.1016/j.jct.2009.11.019.
[46] J.M. Han, H.Y. Shin, B.M. Min, K.H. Han, A. Cho, Measurement and correlation of high pressure phase behavior of carbon dioxide + water system, J. Ind. Eng. Chem. (2009). https://doi.org/10.1016/j.jiec.2008.09.012.
[47] P.J. Carvalho, L.M.C. Pereira, N.P.F. Gonçalves, A.J. Queimada, J.A.P. Coutinho, Carbon dioxide solubility in aqueous solutions of NaCl: Measurements and modeling with electrolyte equations of state, Fluid Phase Equilib. (2015). https://doi.org/10.1016/j.fluid.2014.12.043.
[48] A. Zawisza, B.B. Malesinska, Solubility of carbon dioxide in liquid water and of water in gaseous carbon dioxide in the range 0.2-5 MPa and at temperatures up to 473 K, J. Chem. Eng. Data. 26 (1981) 388–391. https://doi.org/10.1021/je00026a012.
[49] S. Muromachi, A. Shijima, H. Miyamoto, R. Ohmura, Experimental measurements of carbon dioxide solubility in aqueous tetra-n-butylammonium bromide solutions, J. Chem. Thermodyn. (2015). https://doi.org/10.1016/j.jct.2015.01.008.
[50] S.X. Hou, G.C. Maitland, J.P.M. Trusler, Measurement and modeling of the phase behavior of the (carbon dioxide + water) mixture at temperatures from 298.15 K to 448.15 K, J. Supercrit. Fluids. 73 (2013) 87–96. https://doi.org/10.1016/j.supflu.2012.11.011.
[51] R. D'Souza, J.R. Patrick, A.S. Teja, High Pressure Phase Equilibria in the Carbon Dioxide - n-Hexadecane and Carbon Dioxide - Water Systems, Can. J. Chem. Eng. (1988).
[52] S.D. Zaalishvili, The solubility of carbon dioxide mixed with hydrogen and nitrogen in water under pressure, Zh. Fiz. Khim. 14 (1940) 413–417.
[53] F. Lucile, P. Cézac, F. Contamine, J.P. Serin, D. Houssin, P. Arpentinier, Solubility of carbon dioxide in water and aqueous solution containing sodium hydroxide at temperatures from (293.15 to 393.15) K and pressure up to 5 MPa: Experimental measurements, J. Chem. Eng. Data. (2012). https://doi.org/10.1021/je200991x.
[54] L.A. Webster, A.J. Kidnay, Vapor-Liquid Equilibria for the Methane-Propane-Carbon

Dioxide Systems at 230 K and 270 K, J. Chem. Eng. Data. 46 (2001) 759–764. https://doi.org/10.1021/je000307d.
[55] M.B. King, A. Mubarak, J.D. Kim, T.R. Bott, The mutual solubilities of water with supercritical and liquid carbon dioxides, J. Supercrit. Fluids. 5 (1992) 296–302. https://doi.org/https://doi.org/10.1016/0896-8446(92)90021-B.
[56] M. Frost, E. Karakatsani, N. Von Solms, D. Richon, G.M. Kontogeorgis, Vapor-liquid equilibrium of methane with water and methanol. Measurements and modeling, J. Chem. Eng. Data. 59 (2014) 961–967. https://doi.org/10.1021/je400684k.
[57] M. Rigby, J.M. Prausnitz, Solubility of water in compressed nitrogen, argon, and methane, J. Phys. Chem. 72 (1968) 330–334. https://doi.org/10.1021/j100847a064.
[58] A.H. Mohammadi, A. Chapoy, D. Richon, B. Tohidi, Experimental Measurement and Thermodynamic Modeling of Water Content in Methane and Ethane Systems, Ind. Eng. Chem. Res. 43 (2004) 7148–7162. https://doi.org/10.1021/ie049843f.
[59] Y.D. Zel'venskii, Solubility of CO2 in water under pressure, ´Zh. Khim. Prom. 14 (1937) 1250–1257.
[60] S. Mao, Z. Duan, D. Zhang, L. Shi, Y. Chen, J. Li, Thermodynamic modeling of binary CH4–H2O fluid inclusions, Geochim. Cosmochim. Acta. 75 (2011) 5892–5902. https://doi.org/https://doi.org/10.1016/j.gca.2011.07.021.
[61] J. Davalos, W.R. Anderson, R.E. Phelps, A.J. Kidnay, Liquid-vapor equilibria at 250.00.deg.K for systems containing methane, ethane, and carbon dioxide, J. Chem. Eng. Data. 21 (1976) 81–84. https://doi.org/10.1021/je60068a030.
[62] T.A. Al-Sahhaf, A.J. Kidnay, E.D. Sloan, Liquid + vapor equilibriums in the nitrogen + carbon dioxide + methane system, Ind. Eng. Chem. Fundam. 22 (1983) 372–380. https://doi.org/10.1021/i100012a004.
[63] Q. Nasir, K.M. Sabil, K.K. Lau, Measurement of isothermal (vapor+liquid) equilibria, (VLE) for binary (CH4+CO2) from T=(240.35 to 293.15) K and CO2 rich synthetic natural gas systems from T=(248.15 to 279.15) K, J. Nat. Gas Sci. Eng. 27 (2015) 158–167. https://doi.org/https://doi.org/10.1016/j.jngse.2015.08.045.
[64] F.A. Somait, A.J. Kidnay, Liquid-vapor equilibriums at 270.00 K for systems containing nitrogen, methane, and carbon dioxide, J. Chem. Eng. Data. 23 (1978) 301–305. https://doi.org/10.1021/je60079a019.
[65] N. Xu, J. Dong, Y. Wang, J. Shi, High pressure vapor liquid equilibria at 293 K for systems containing nitrogen, methane and carbon dioxide, Fluid Phase Equilib. 81 (1992) 175–186. https://doi.org/https://doi.org/10.1016/0378-3812(92)85150-7.
[66] M.J. Huron, J. Vidal, New mixing rules in simple equations of state for representing vapour-liquid equilibria of strongly non-ideal mixtures, Fluid Phase Equilib. (1979). https://doi.org/10.1016/0378-3812(79)80001-1.
[67] K.S. Pedersen, J. Milter, C.P. Rasmussen, Mutual solubility of water and a reservoir fluid at high temperatures and pressures, Fluid Phase Equilib. 189 (2001) 85–97. https://doi.org/10.1016/s0378-3812(01)00562-3.
[68] A. Austegard, E. Solbraa, G. de Koeijer, J. Molnkiv, Thermodynamic Models for Calculating Mutual Solubilities in H2O-CO2-CH4 mixtures, Chem. Eng. Res. Des. 84 (2006).
[69] G.M. Kontogeorgis, E.C. Voutsas, I. V. Yakoumis, D.P. Tassios, An Equation of State for Associating Fluids, Ind. Eng. Chem. Res. 35 (1996) 4310–4318. https://doi.org/10.1021/ie9600203.
[70] G.M. Kontogeorgis, I. V Yakoumis, H. Meijer, E. Hendriks, T. Moorwood,

Multicomponent phase equilibrium calculations for water–methanol–alkane mixtures, Fluid Phase Equilib. 158–160 (1999) 201–209. https://doi.org/https://doi.org/10.1016/S0378-3812(99)00060-6.
[71] A. Valtz, A. Chapoy, C. Coquelet, P. Paricaud, D. Richon, Vapour–liquid equilibria in the carbon dioxide–water system, measurement and modelling from 278.2 to 318.2K, Fluid Phase Equilib. 226 (2004) 333–344. https://doi.org/https://doi.org/10.1016/j.fluid.2004.10.013.
[72] Z.L. Yang, H.Y. Yu, Z.W. Chen, S.Q. Cheng, J.Z. Su, A compositional model for CO2 flooding including CO2 equilibria between water and oil using the Peng–Robinson equation of state with the Wong–Sandler mixing rule, Pet. Sci. (2019). https://doi.org/10.1007/s12182-018-0294-2.
[73] J. Gernert, R. Span, EOS-CG: A Helmholtz energy mixture model for humid gases and CCS mixtures, J. Chem. Thermodyn. 93 (2016) 274–293. https://doi.org/10.1016/j.jct.2015.05.015.
[74] S. Herrig, New Helmholtz-Energy Equations of State for Pure Fluids and CCS-Relevant Mixtures, (2018) 260.
[75] A. Aasen, M. Hammer, G. Skaugen, J.P. Jakobsen, Ø. Wilhelmsen, Thermodynamic models to accurately describe the PVTxy-behavior of water / carbon dioxide mixtures, Fluid Phase Equilib. 442 (2017) 125–139.
[76] C.H. Twu, D. Bluck, J.R. Cunningham, J.E. Coon, A cubic equation of state with a new alpha function and a new mixing rule, Fluid Phase Equilib. 69 (1991) 33–50. https://doi.org/10.1016/0378-3812(91)90024-2.
[77] M.-J. Huron, J. Vidal, New mixing rules in simple equations of state for representing vapour-liquid equilibria of strongly non-ideal mixtures, Fluid Phase Equilib. 3 (1979) 255–271. https://doi.org/https://doi.org/10.1016/0378-3812(79)80001-1.
[78] D.S.H. Wong, S.I. Sandler, A theoretically correct mixing rule for cubic equations of state, AIChE J. 38 (1992) 671–680. https://doi.org/10.1002/aic.690380505.
[79] E. Petropoulou, G.D. Pappa, E. Voutsas, Fluid Phase Equilibria Modelling of phase equilibrium of natural gas mixtures containing associating compounds, Fluid Phase Equilib. 433 (2017) 135–148. https://doi.org/10.1016/j.fluid.2016.10.028.
[80] N. Von Solms, M.L. Michelsen, G.M. Kontogeorgis, Computational and Physical Performance of a Modified PC-SAFT Equation of State for Highly Asymmetric and Associating Mixtures, Ind. Eng. Chem. Res. 42 (2003) 1098–1105. https://doi.org/10.1021/ie020753p.
[81] O. Kunz, W. Wagner, The GERG-2008 Wide-Range Equation of State for Natural Gases and Other Mixtures: An Expansion of GERG-2004, J. Chem. Eng. Data. 57 (2012) 3032–3091. https://doi.org/10.1021/je300655b.
[82] E. Voutsas, K. Magoulas, D. Tassios, Universal mixing rule for cubic equations of state applicable to symmetric and asymmetric systems: Results with the Peng-Robinson equation of state, Ind. Eng. Chem. Res. 43 (2004) 6238–6246. https://doi.org/10.1021/ie049580p.
[83] E. Collinet, J. Gmehling, Prediction of phase equilibria with strong electrolytes with the help of the volume translated Peng-Robinson group contribution equation of state (VTPR), Fluid Phase Equilib. (2006). https://doi.org/10.1016/j.fluid.2006.05.033.
[84] Z.-L. Yang, H.-Y. Yu, Z.-W. Chen, S.-Q. Cheng, J.-Z. Su, A compositional model for CO2 flooding including CO2 equilibria between water and oil using Peng-Robinson equation of state with Wong-Sandler mixing rule, Pet. Sci. (2019) 1–16.

[85] A. Chapoy, R. Burgass, A. Terrigeol, C. Coquelet, Water Content of CO 2 -rich Mixtures: Measurements and Modeling using the Cubic-Plus-Association Equation of State , J. Nat. Gas Eng. 1 (2016) 85–97. https://doi.org/10.7569/jnge.2015.692505.
[86] I. Tsivintzelis, S. Ali, G.M. Kontogeorgis, Modeling phase equilibria for acid gas mixtures using the cubic-plus-association equation of state. 3. Applications relevant to liquid or supercritical CO2 transport, J. Chem. Eng. Data. 59 (2014) 2955–2972. https://doi.org/10.1021/je500090q.
[87] P. Reshadi, K.H. Nasrifar, M. Moshfeghian, Evaluating the phase equilibria of liquid water+natural gas mixtures using cubic equations of state with asymmetric mixing rules, Fluid Phase Equilib. 302 (2011) 179–189. https://doi.org/10.1016/j.fluid.2010.08.007.
[88] K.Y.S.K.R.C.W.G.C. Wael A. Fouad Matt Yarrison, High Pressure Measurements and Molecular Modeling of the Water Content of Acid Gas Containing Mixtures, AIChE J. (2015).
[89] K. Nasrifar, F. Alavi, J. Javanmardi, Prediction of water content of natural gases using the PC-SAFT equation of state, Fluid Phase Equilib. 453 (2017) 40–45. https://doi.org/https://doi.org/10.1016/j.fluid.2017.08.023.
[90] V. Papaioannou, F. Calado, T. La, S. Dufal, M. Sadeqzadeh, G. Jackson, C.S. Adjiman, A. Galindo, Application of the SAFT- g Mie group contribution equation of state to fl uids of relevance to the oil and gas industry, 416 (2016) 104–119. https://doi.org/10.1016/j.fluid.2015.12.041.
[91] H. Zhao, Modeling vapor-liquid phase equilibria of methane-water and methane-carbon dioxide-water systems at 274K to 573K and 0.1 to 150 MPa using PRSV equation of state and Wong-Sandler mixing rule, Fluid Phase Equilib. 447 (2017) 12–26. https://doi.org/10.1016/j.fluid.2017.05.015.
[92] H. Zhao, S.N. Lvov, Phase behavior of the CO2–H2O system at temperatures of 273–623 K and pressures of 0.1–200 MPa using Peng-Robinson-Stryjek-Vera equation of state with a modified Wong-Sandler mixing rule: An extension to the CO2–CH4–H2O system, Fluid Phase Equilib. 417 (2016) 96–108. https://doi.org/https://doi.org/10.1016/j.fluid.2016.02.027.
[93] J.M. Míguez, M.C. Dos Ramos, M.M. Piñeiro, F.J. Blas, An examination of the ternary methane + carbon dioxide + water phase diagram using the SAFT-VR approach, J. Phys. Chem. B. 115 (2011) 9604–9617. https://doi.org/10.1021/jp2017488.
[94] A. Chapoy, R. Burgass, B. Tohidi, J.M. Austell, C. Eickhoff, Effect of Common Impurities on the Phase Behavior of Carbon-Dioxide-Rich Systems: Minimizing the Risk of Hydrate Formation and Two-Phase Flow, SPE J. 16 (2011) 921–930. https://doi.org/10.2118/123778-PA.
[95] A. Chapoy, H. Haghighi, R. Burgass, B. Tohidi, On the phase behaviour of the (carbon dioxide + water) systems at low temperatures: Experimental and modelling, J. Chem. Thermodyn. 47 (2012) 6–12. https://doi.org/10.1016/j.jct.2011.10.026.
[96] P.M. Mathias, T.W. Copeman, Extension of the Peng-Robinson equation of state to complex mixtures: Evaluation of the various forms of the local composition concept, Fluid Phase Equilib. 13 (1983) 91–108.
[97] J.-N. Jaubert, F. Mutelet, VLE predictions with the Peng–Robinson equation of state and temperature dependent kij calculated through a group contribution method, Fluid Phase Equilib. 224 (2004) 285–304. https://doi.org/https://doi.org/10.1016/j.fluid.2004.06.059.

[98] J.N. Jaubert, R. Privat, Relationship between the binary interaction parameters (kij) of the Peng-Robinson and those of the Soave-Redlich-Kwong equations of state: Application to the definition of the PR2SRK model, Fluid Phase Equilib. (2010). https://doi.org/10.1016/j.fluid.2010.03.037.
[99] J. Gernert, R. Span, EOS–CG: A Helmholtz energy mixture model for humid gases and CCS mixtures, J. Chem. Thermodyn. 93 (2016) 274–293. https://doi.org/https://doi.org/10.1016/j.jct.2015.05.015.
[100] Z. Duan, S. Mao, A thermodynamic model for calculating methane solubility, density and gas phase composition of methane-bearing aqueous fluids from 273 to 523K and from 1 to 2000bar, Geochim. Cosmochim. Acta. 70 (2006) 3369–3386. https://doi.org/https://doi.org/10.1016/j.gca.2006.03.018.
[101] R. Burgass, A. Chapoy, B. Tohidi, Experimental and Modelling Low Temperature Water Content in Multicomponent Gas Mixtures, in: Proceeding 7th Int. Conf. Gas Hydrates (ICGH 2011), Edinburgh, 2011.
[102] A. Chapoy, R. Brugrass, B. Tohidi, J.M. Austell, C. Eickhoff, Effect of Common Impurities on the Phase Behaviour of Carbon-Dioxide-Rich Systems: Minimizing the Risk of Hydrate Formation and Two-Phase Flow, SPE J. SPE-123778 (2011).
[103] H. Haghighi, A. Chapoy, R. Burgass, B. Tohidi, on the Phase Behaviour of the Carbon Dioxide - Water Systems At Low Temperatures, Icgh 2011. 44 (2011).
[104] P. Ahmadi, A. Chapoy, CO 2 solubility in formation water under sequestration conditions, Fluid Phase Equilib. 463 (2018) 80–90. https://doi.org/10.1016/j.fluid.2018.02.002.
[105] A. Chapoy, R. Burgass, A. Terrigeol, C. Coquelet, Water Content of CO2 rich Mixtures: Measurements and Modeling using the Cubic-Plus-Association Equation of State, J. Nat. Gas Eng. 1 (2016) 85–97. https://pdfs.semanticscholar.org/e45d/e7c3f6bc55d830d0058e4ade64d141b120f0.pdf?_ga=2.159672189.1728404663.1563924027-567500309.1563924027.